

People's Democratic Republic of Algeria
Ministry of Higher Education and Scientific Research
University M'Hamed BOUGARA – Boumerdès



Institute of Electrical and Electronic Engineering
Department of power and control engineering

Project Report Presented in Partial Fulfilment of
the Requirements of the Degree of

'MASTER 2'
In Power Engineering

Title:

**FPGA based DC motor speed and torque
control**

Presented By:

- **BOUAOU Djameleddine**
- **SOUISSI Slimane**

Supervisor:

- **Pr. BENTARZI.**

Registration Number :/2019

Abstract

This project describes a design and implementation of an FPGA based speed and torque control of a direct current motor.

The speed and torque are controlled using the armature voltage variation technique. A dual H-bridge integrated circuit motor driver (L293D) is used to drive a separately excited DC motor. An Altera FPGA DE2 board is used to implement the digital controllers that regulate both the voltage and the armature current and hence the speed and torque.

In general, the output speed of the DC motor is measured and compared with a reference. Thus, the armature voltage is continually adjusted to keep the measured speed as the reference while the load varies.

Dedication

To my beloved parents.

To my brothers Mahdi & Chems-Eddine.

To all my family without forgetting my INELEC family.

To all my friends and everybody with whom I exchanged a smile.

To all these I dedicate this modest work.

Slimane

I would like to take this opportunity to say warm thanks to all my beloved friends.

To my mom "Nassima", To my dad "Zineddine,

Whose constant encouragement, limitless giving and great sacrifice, helped me accomplish my degree.

To my sister and her husband "Yasmine and Ferhat"

To my brother "Ryad"

To all my aunts,

For their generous support they provided me throughout my entire life and particularly through the process of pursuing the master degree. Because of their unconditional love and prayers, I have the chance to complete this project.

To Walid my best friend, who has been so supportive along the way of doing my report.

I am very appreciative to my classmates at INELEC,

I am also grateful to all my instructors at INELEC since the 1st year.

Last but not least, deepest thanks go to all people who took part in making this project real.

Djameleddine.

Acknowledgements

In the Name of Allah, the Most Merciful, the Most Compassionate all praise be to Allah, the Lord of the worlds; and prayers and peace be upon Mohamed His servant and messenger.

First and foremost, we must acknowledge our limitless thanks to Allah, the Ever-Magnificent; the Ever-Thankful, for His helps and bless. We are very sure that this work would have never become true, without His guidance.

We owe a deep debt of gratitude to our institute for giving us an opportunity to complete this work.

We are grateful to some people, who worked hard with us from the beginning until the completion of the present project particularly our supervisor Pr. Hamid BENTARZI.

Table of contents:

Abstract	
Dedication	II
Acknowledgements.....	III
General Introduction	1
<i>Chapter I:</i> DC motor overview.....	2
I.1 DC Machinery fundamentals	2
I.2 DC motor:.....	2
I.2.1 History:.....	2
I.2.2 Definition of the DC motor:.....	3
I.2.3 DC Motor major components:	4
I.2.4 DC Motor working principle:	5
I.2.5 DC motor equivalent circuit:	7
I.2.6 DC Motor types:	8
<i>Chapter II:</i> DC motor modelling.....	9
II.1 Introduction	9
II.2 The Dynamic model of the DC motor:.....	9
II.3 Stability Study.....	11
II.3.1 DC Motor stability checking	12
II.4 DC Motor parameters identification	12
II.4.1 Identifying R_a and L_a :	13
II.4.2 Identifying K_g :.....	15
II.4.3 Identifying B :	16
II.4.4 Identifying J :.....	17
<i>Chapter III:</i> DC Motor open and closed loop control.....	19
III.1 Speed and torque characteristics and control:.....	19
III.1.1 Armature resistance control.....	20
III.1.2 Field flux ϕ control:	21
III.1.3 Armature voltage control:	23
III.2 Operation modes:.....	24
III.3 Open loop control:	25
III.3.1 DC choppers:	26

III.4	Closed loop control:	29
III.5	Separately excited DC motor drive:	30
III.5.1	Motor Transfer Function.....	30
III.5.2	Power converter transfer function:	33
III.5.3	The speed controller:	34
III.6	Closed-loop speed control.....	34
III.7	The closed-loop current (torque) control.....	36
<i>Chapter IV: Simulation of the control system.....</i>		<i>38</i>
IV.1	SIMULINK model of the control system:.....	38
IV.2	The controller parameters tuning:	38
IV.3	PID tuner:	39
IV.4	Simulation results:	40
<i>Chapter V: Hardware design and implementation.....</i>		<i>43</i>
V.1	FPGA hardware blocks:	43
V.1.1	ADC block:.....	43
V.1.2	PWM block:	44
V.1.3	PID algorithm:	45
V.1.4	Clock divider block:	47
V.1.5	Seven segment display block:	47
V.2	Off board design:	49
V.2.1	The actual speed and current acquisition:	49
V.2.2	Analog to digital conversion:.....	49
V.3	Hardware implementation:	50
V.3.1	Experimental setup :	51
V.3.2	Implementation results:	52
General Conclusion.....		54
References		55
Appendix A		56

List of tables:

Table II-1. DC test values.	13
Table II-2. AC test values	14
Table II-3. Back emf and their corresponding motor mechanical speed data.....	16
Table II-4. DC Motor parameters.....	18
Table V-1. Result of control system for various reference speeds.....	53

List of figures :

Figure I-1. A simple rotating loop between curved pole faces.	2
Figure I-2. A scheme of a universal DC Motor.....	5
Figure I-3. DC Motor equivalent circuit.	7
Figure I-4. The simplified equivalent circuit of DC Motor.....	7
Figure II-1. The armature of a separately excited DC motor.	9
Figure II-2. the injected voltage versus the measured current graph	13
Figure II-3. The AC injected voltage versus the AC measured current	15
Figure II-4. Back emf versus mechanical speed graph	16
Figure III-1. The impact of varying the armature resistance on the mechanical speed.	20
Figure III-2. The effect of increasing the flux on the mechanical speed.....	22
Figure III-3. The impact of increasing the armature voltage on the mechanical speed.	23
Figure III-4. The DC motor four quadrant modes[3].	25
Figure III-5. A DC to DC Scheme of a DC chopper[3].	26
Figure III-6. Equivalent circuit of a DC motor connected to a DC chopper [3].	27
Figure III-7. The equivalent circuit when the switch S is closed[3].	28
Figure III-8. The equivalent circuit when the switch S is open [3].....	28
Figure III-9. Block diagram of a closed- loop speed control system.	30
Figure III-10. Separately excited DC motor block diagram.....	31
Figure III-11. Simplified block diagram for DC motor.	33
Figure III-12. PWM ganeration.....	33
Figure III-13. Speed control-loop block diagram.....	34
Figure III-14. Speed and current (torque) control block diagram.	36
Figure III-15. Current (torque) control loop block diagram.....	37
Figure IV-1. SIMULINK block diagram.	38
Figure IV-2. PI speed controller parameters.	39
Figure IV-3. PI current (torque) controller parameters.	40
Figure IV-4 speed waveform with $w_r = 100$ rpm.....	40
Figure IV-5. Armature current waveform at full load.....	41
Figure V-1. ADC VHDL block.....	43
Figure V-2. PWM VHDL block.....	44
Figure V-3. PWM flowchart	45
Figure V-4. PID flowchart.	46
Figure V-5. Clock divider VHDL block	47
Figure V-6. Seven segment display VHDL block.....	47
Figure V-7. VHDL blocks interconnection.....	48
Figure V-8. Hardware system connections.	50
Figure V-9. Experimental setup connections.	51
Figure V-10. Measured tacho-generator voltage (speed) vs time.	53

General Introduction

Direct current motors have been the backbone of industrial applications. Ever since the Industrial Revolution., it has been widely used in automotive, manufacturing, automation, stepper drives. This is due to the motor's high performance and easy speed control.

Conventionally, analog controllers based on operational amplifiers have been used to implement earlier control systems. With rapid advances in control technology, most of the industrial control systems include digital controllers.

FPGA based digital controller have become the most favorable prototyping digital systems. The control algorithms are developed in VHDL, which is now one of the most popular standard digital hardware description languages.

In a digital motor drive control system, the motor speed and motor current are measured by proper sensors and the output signals from these sensors are sent to the controller as feedback signals. The controller generates the control signal to the power converter based on the reference and feedback signals.

I.1 DC Machinery fundamentals

DC machines are generators that convert mechanical energy to electric energy and motors that convert an electric energy to mechanical energy. Most DC machines are like AC machines in that they have AC voltages and currents within them.

DC machines have a DC output only because a mechanism exists that converts the internal AC voltages at their terminals. This mechanism is called a commutator, DC machinery is also known as commutating machinery.

The fundamental principles involved in the operation of de machines are very simple. Unfortunately, they are usually somewhat obscured by the complicated construction of real machines.

DC motors are DC machines used as motors, and DC generators are DC machines used as generators. The same physical machine can operate as either a motor or a generator; it is simply a question of the direction of the power now through it [1].

The simplest possible rotating dc machine is shown in Figure 1.1. It consists of a single loop of wire rotating about a fixed axis. The rotating part of this machine is called the rotor, and the stationary part is called the stator. The magnetic field for the machine is supplied by the magnetic north and south poles on the stator as shown in Figure I-1.

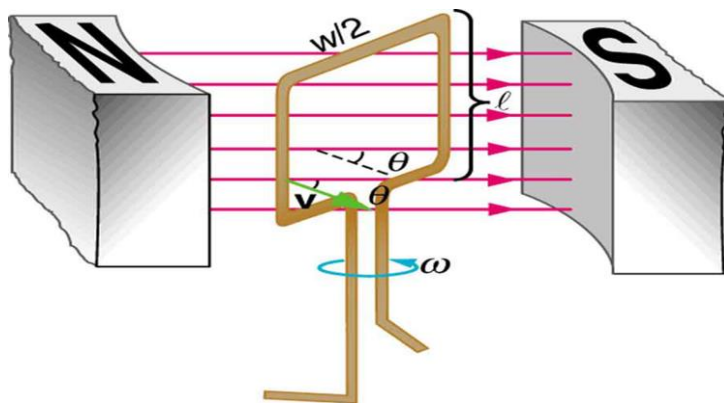


Figure I-1. A simple rotating loop between curved pole faces.

I.2 DC motor:**I.2.1 History:**

The earliest power systems in the United States were DC systems, but by the 1890s AC power systems were clearly winning out over DC systems. Despite this fact, DC motors

continued to be a significant fraction of the machinery purchased each year through the 1960s. However, that fraction has declined in the last 40 years.

There were several reasons for the continued popularity of DC motors. One was that DC power systems are still common in cars, trucks, and aircraft. When a vehicle has a DC power system, it makes sense to consider using DC motors. Another application for DC motors was a situation in which wide variations in speed are needed. Before the widespread use of power electronic rectifier-inverters, DC motors were unexcelled in speed control applications. Even if no DC power source were available, solid-state rectifier and chopper circuits were used to create the necessary DC power, and DC motors were used to provide the desired speed control [1].

I.2.2 Definition of the DC motor:

A DC motor is any of a class of rotary electrical machines that converts direct current electrical energy into mechanical energy. The most common types rely on the forces produced by magnetic fields. Nearly all types of DC motors have some internal mechanism, either electromechanical or electronic; to periodically change the direction of current flow in part of the motor.

DC motors were the first type widely used, since they could be powered from existing direct-current lighting power distribution systems. A DC motor's speed can be controlled over a wide range, using either a variable supply voltage or by changing the strength of current in its field windings. Small DC motors are used in tools, toys, and appliances. The universal motor can operate on direct current but is a lightweight brushed motor used for portable power tools and appliances. Larger DC motors are used in propulsion of electric vehicles, elevator and hoists, or in drives for steel rolling mills. The advent of power electronics has made replacement of DC motors with AC motors possible in many applications.

DC motors are often compared by their speed regulations. The speed regulation (SR) of a motor is defined by:

$$SR = \frac{\omega_{nl} - \omega_{fl}}{\omega_{fl}} \times 100\% \quad (I.1)$$

Where:

- ω_{nl} is the no load speed of the DC motor.
- ω_{fl} is the full load speed of the DC motor.

It is a rough measure of the shape of a motor's torque- speed characteristic; a positive speed regulation means that a motor's speed drops with increasing load, and a negative speed regulation means a motor's speed increases with increasing load. The magnitude of the speed regulation tells approximately how steep the slope of the torque- speed curve is.

I.2.3 DC Motor major components:

DC motors are made up of several major components which include the following:

- **Frame:** the frame is where the armature is placed and the field coils are mounted.
- **Shaft:** is the rotating part where the converted electrical energy is extracted as mechanical energy to be used by coupling it to other machines such as an induction motor.
- **Bearings:** the bearings in an electric motor are used to support and locate the rotor, to keep the air gap small and consistent and transfer the loads from the shaft to the motor. The bearings should be able to operate at low and high speeds whilst minimizing frictional losses.
- **Main Field Windings (Stator):** in large motors used in industrial applications the stator is an electromagnet. When voltage is applied to stator windings an electromagnet with north and south poles is established. The resultant magnetic field is static (non-rotational).
- **Armature (Rotor):** the armature rotates between the poles of the field windings. The armature is made up of a shaft, core, armature windings, and a commutator. The armature windings are usually form wound and then placed in slots in the core.
- **Commutator:** are the device used in the process of switching the field in the armature windings to produce constant torque in one direction, it is connected to the armature, which enables this switching of current.
- **Brush Assembly:** brushes ride on the side of the commutator to provide supply voltage to the motor. The DC motor is mechanically complex which can cause problems for them in certain adverse environments. Dirt on the commutator, for example, can inhibit supply voltage from reaching the armature. A certain amount of care is required when using DC motors in certain industrial applications. Corrosives can damage the commutator. In addition, the action of the carbon brush against the commutator causes sparks which may be problematic in hazardous environments.

FigureI-2 shown below illustrates a universal scheme of a DC Motor.

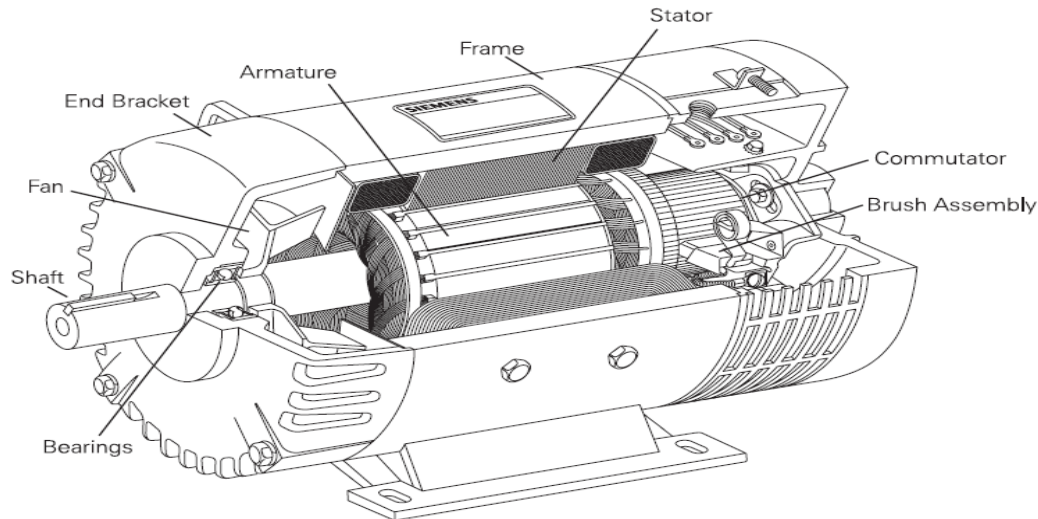


Figure I-2. A scheme of a universal DC Motor.

I.2.4 DC Motor working principle:

Consider a coil in a magnetic field of flux density B . When the two ends of the coil are connected across a DC voltage source, current I flows through it. A force is exerted on the coil as a result of the interaction of magnetic field and electric current. The force on the two sides of the coil is such that the coil starts to move in the direction of force.

In an actual DC motor, several such coils are wound on the rotor, all of which experience force, resulting in rotation. The greater the current in the wire, or the greater the magnetic field, the faster the wire moves because of the greater force created.

At the same time this torque is being produced, the conductors are moving in a magnetic field. At different positions, the flux linked with it changes, which causes an emf to be induced ($e = d\phi/dt$). This voltage is in opposition to the voltage that causes current flow through the conductor and is referred to as a counter-voltage or back emf.

The value of current flowing through the armature is dependent upon the difference between the applied voltage and this counter-voltage. The current due to this counter-voltage tends to oppose the very cause for its production according to Lenz's law. It results in the rotor slowing down. Eventually, the rotor slows just enough so that the force created by the magnetic field equals the load force applied on the shaft. Then the system moves at constant velocity.

I.2.4.1 Torque and power

The equation for torque developed in a DC motor can be derived as follows:

The force on one coil of wire is given by:

$$\mathbf{F} = i \mathbf{l} \times \mathbf{B} \quad [\text{N}] \quad (\text{I.2})$$

Where: l and B are vector quantities

- l is the length of the wire and B is the magnetic field.

Since: $\mathbf{B} = \boldsymbol{\phi}/\mathbf{A}$.

Where A is the area of the coil.

Therefore the torque for a multi turn coil with an armature current of I_a :

$$\mathbf{T}_e = K \boldsymbol{\phi} I_a \quad (\text{I.3})$$

Where ϕ is the flux/pole in weber, K is a constant depending on coil geometry which lumps all the constant parameters (number of turns of the coil, length ...etc.), and I_a is the current flowing in the armature winding.

The mechanical power generated is the product of the machine torque and the mechanical speed of rotation $\boldsymbol{\omega}_m$.

$$P_m = \boldsymbol{\omega}_m T \quad (\text{I.4})$$

I.2.4.2 Back emf

Due to the rotation of this coil in the magnetic field, the flux linked with it changes at different positions, which causes an emf to be induced.

The induced emf in a single coil is:

$$e = d\boldsymbol{\phi}_c/dt$$

Since the flux linking the coil is:

$$\boldsymbol{\phi}_c = \boldsymbol{\phi} \sin(\boldsymbol{\omega}_c t)$$

Thus, the induced voltage is:

$$e = \boldsymbol{\phi} \boldsymbol{\omega} \cos(\boldsymbol{\omega}_c t) \quad (\text{I.5})$$

Note that equation (1.5) gives the emf induced in one coil. As there are several coils wound all around, the rotor, each with a different emf depending on the amount of flux change through it, the total emf may be obtained by summing up the individual emfs. The total emf induced in the motor by several such coils wound on the rotor can be obtained by integrating equation (1.5) over the time, and expressed as:

$$e_b = K \boldsymbol{\phi} \boldsymbol{\omega}_m \quad (\text{I.6})$$

The electrical power generated by the machine is given by:

$$P_d = e_b I_a$$

Thus,

$$P_d = K \boldsymbol{\phi} \boldsymbol{\omega}_m I_a \quad (\text{I.7})$$

I.2.5 DC motor equivalent circuit:

As Figure I-3 illustrates, the armature circuit is represented by an ideal voltage source E_A and a resistor R_A . This representation is really the Thevenin equivalent of the entire rotor structure, including rotor coils, interpoles, and compensating windings, if present. The brush voltage drop is represented by a small battery V_{brush} opposing the direction of current flow in the machine. Inductor L_F and resistor R_F represent the field coils, which produce the magnetic flux in the generator. The separate resistor R_{adj} represents an external variable resistor used to control the amount of current in the field circuit.

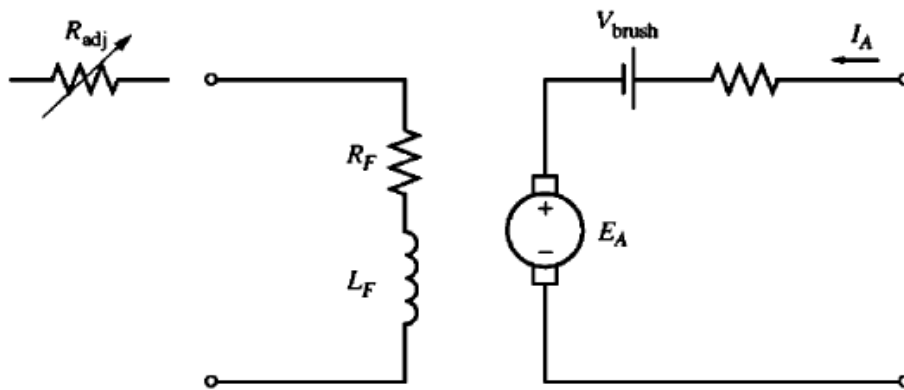


Figure I-3. DC Motor equivalent circuit.

There are a few variations and simplifications of this basic equivalent circuit. The brush drop voltage is often only a very tiny fraction of the generated voltage in a machine. Therefore, in cases where it is not too critical, the brush drop voltage may be left out or approximately included in the value of R_A . Also, the internal resistance of the field coils is sometimes lumped together with the variable resistor, and the total is called R_F (see Figure I-4). A third variation is that some generators have more than one field coil, all of which will appear on the equivalent circuit.

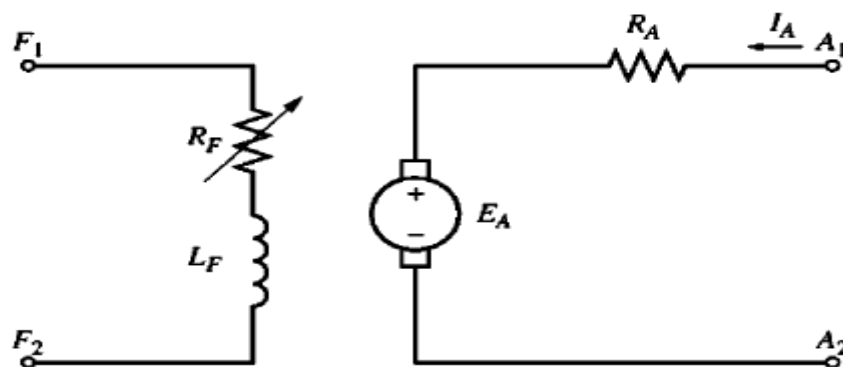


Figure I-4. The simplified equivalent circuit of DC Motor.

I.2.6 DC Motor types:

There are five major types of DC motors in general use, this classification is based on the connection of both the stator and the rotor, and those types are:

- **The separately excited DC motor:** A separately excited dc motor is a motor whose field circuit is supplied from a separate constant-voltage power supply. However, the armature is supplied from a variable controlled DC source.
- **The shunt DC motor:** In a shunt motor the field is connected in parallel (shunt) with the armature windings. The shunt-connected motor offers good speed regulation. The shunt-connected motor offers simplified control for reversing. This is especially beneficial in regenerative drives.
- **The permanent-magnet DC motor:** the permanent magnet motor uses a magnet to supply field flux. Permanent magnet DC motors have excellent starting torque capability with good speed regulation. A disadvantage of permanent magnet DC motors is they are limited to the amount of load they can drive. These motors can be found on low horsepower applications. Another disadvantage is that torque is usually limited to 150% of rated torque to prevent demagnetization of the permanent magnets.
- **The series DC motor:** In a series DC motor the field is connected in series with the armature. The field is wound with a few turns of large wire because it must carry the full armature current. A characteristic of series motors is the motor develops a large amount of starting torque. However, speed varies widely between no load and full load. Series motors cannot be used where a constant speed is required under varying loads. Additionally, the speed of a series motor with no load increases to the point where the motor can become damaged. Some load must always be connected to a series-connected motor. Series-connected motors generally are not suitable for use on most variable speed drive applications.
- **The compound DC motor:** Compound motors have a field connected in series with the armature and a separately excited shunt field. The series field provides better starting torque and the shunt field provides better speed regulation. However, the series field can cause control problems in variable speed drive applications and is generally not used in four quadrant drives.

II.1 Introduction

The modelling of a DC motor is a very important step in controlling its speed and torque, in this chapter, the dynamic equations of torque and speed are to be developed in addition to the parameters of the used DC motor.

The separately excited DC motor as defined in the previous chapter is the DC motor used in this project, since the field circuit is supplied from a constant source then the field current I_f and the magnetic field is always constant, thus, the parameters of the field circuit (i.e. L_f and R_f) are to be neglected.

Hence, in this project all the studies are to be held on the armature only.

II.2 The Dynamic model of the DC motor:

Figure II-1 shown below represents the armature of a DC motor.

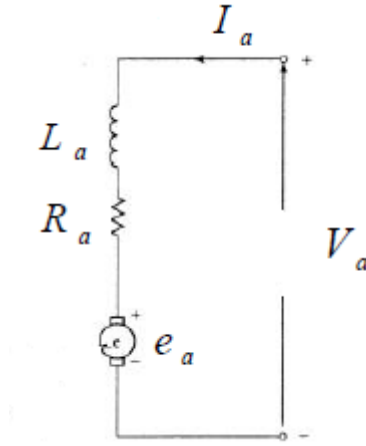


Figure II-1. The armature of a separately excited DC motor.

Applying Kirchhoff's law on the circuit shown above:

$$V_a = I_a R_a + L_a \frac{dI_a}{dt} + e_a$$

Thus;

$$\frac{dI_a}{dt} = \frac{V_a}{L_a} - \frac{I_a R_a}{L_a} - \frac{e_a}{L_a} \quad (\text{II.1})$$

Applying the motion equation on the circuit shown above:

$$T_e = J \frac{d\omega_m}{dt} + B\omega_m + T_L$$

Thus;

$$\frac{d\omega_m}{dt} = \frac{T_e}{J} - \frac{B\omega_m}{J} - \frac{T_L}{J} \quad (\text{II.2})$$

As mentioned previously, this project is about a separately excited DC motor, hence, the equations (I.3) and (I.6) could be rearranged as:

$$T_e = K_g I_a \quad (\text{II.3})$$

$$e_a = K_g \omega_m \quad (\text{II.4})$$

Where K_g is the product of the constants K and ϕ and is called the motor constant.

Replacing (II.3) and (II.4) in (II.1) and (II.2) and rearranging it. Hence, the system differential equations are as the following:

$$\begin{cases} \frac{dI_a}{dt} = \frac{V_a}{L_a} - \frac{I_a R_a}{L_a} - \frac{K_g}{L_a} \omega_m \\ \frac{d\omega_m}{dt} = \frac{K_g}{J} I_a - \frac{B\omega_m}{J} - \frac{T_L}{J} \end{cases} \quad (\text{II.5})$$

Introducing LAPLACE transform in the previous differential equations to get:

$$\begin{cases} sI_a = -\frac{R_a}{L_a} I_a + \frac{1}{L_a} V_a - \frac{K_g}{L_a} \omega_m \\ s\omega_m = \frac{K_g}{J} I_a - \frac{B}{J} \omega_m - \frac{1}{J} T_L \end{cases} \quad (\text{II.6})$$

Where:

- S is the Laplacian differential operator with respect of time.
- L_a and R_a are the inductor and the resistor of the armature respectively.
- V_a is the controlled DC source feeding the armature.
- J is the moment of inertia of the load [$kg^2 m^2 / s^2$].
- B is the viscous friction (N.m/rad/s)
- I_a , e_a and ω_m are defined in the previous chapter.

Equations (II.6) may be cast under a state-space form, this form represents the state-space model of the DC Motor such as:

$$\begin{bmatrix} sI_a \\ s\omega_m \end{bmatrix} = \begin{bmatrix} -\frac{R_a}{L_a} & -\frac{K_g}{L_a} \\ \frac{K_g}{J} & -\frac{B}{J} \end{bmatrix} \begin{bmatrix} I_a \\ \omega_m \end{bmatrix} + \begin{bmatrix} \frac{1}{L_a} & 0 \\ 0 & -\frac{1}{J} \end{bmatrix} \begin{bmatrix} V_a \\ T_L \end{bmatrix} \quad (\text{II.7})$$

Writing the equation (II.7) in compact form:

$$\mathbf{X} = \mathbf{A}\dot{\mathbf{X}} + \mathbf{B}\mathbf{U}$$

Where:

- A represents the system matrix.
- X represents the state-variable vector.
- B represents the control matrix.
- U represents the input vector.

II.3 Stability Study

Stability is mostly concerned with dynamical systems. It is a fundamental requirement in most engineering applications that the systems designed are stable. In control engineering applications, the design of a control system must first guarantee the stability of the overall system.

When a system is unstable, the output of the system may be infinite even though the input to the system was finite. This causes a number of practical problems. Also, systems that are unstable often incur a certain amount of physical damages, which can become costly.

In other words, the stability of any system is the degree to which the system may resist changes or at least go back to its steady state operation. The different kinds of stability are defined based on how the system goes back to normal when perturbed.

A DC Motor is said to be in equilibrium if the torque developed by the motor is exactly equal to the load torque. If the DC Motor comes out of the state of equilibrium due to some disturbance, it comes back to steady state for stable equilibrium but for unstable equilibrium the speed of the DC Motor increases uncontrollably or decreases to zero.

II.3.1 DC Motor stability checking

For stability checking purpose, the roots of the system are to be calculated and their real part must be negative; the eigen values of the system matrix **A** are the roots of the system and they are obtained by solving the following equation:

$$\det(\lambda \mathbf{I} - \mathbf{A}) = 0 \quad (\text{II.8})$$

Where **I** is the 2x2 identity matrix such as: $\begin{bmatrix} 1 & 0 \\ 0 & 1 \end{bmatrix}$

Solving the equation (II.8) for the unknown λ :

$$\lambda_1 = -\frac{1}{2} \left(\frac{R_a}{L_a} + \frac{B}{J} \right) + \frac{1}{2} \sqrt{\left(\frac{R_a}{L_a} + \frac{B}{J} \right)^2 - 4 \left(\frac{R_a B}{L_a J} + \frac{K_g^2}{L_a J} \right)} \quad (\text{II.9})$$

$$\lambda_2 = -\frac{1}{2} \left(\frac{R_a}{L_a} + \frac{B}{J} \right) - \frac{1}{2} \sqrt{\left(\frac{R_a}{L_a} + \frac{B}{J} \right)^2 - 4 \left(\frac{R_a B}{L_a J} + \frac{K_g^2}{L_a J} \right)} \quad (\text{II.10})$$

As noticed in equations (II.9) and (II.10) the real part of the roots are the same in both λ_1 and λ_2 and since R_a, L_a, B and J are all positive so:

$$-\frac{1}{2} \left(\frac{R_a}{L_a} + \frac{B}{J} \right) < 0$$

As a conclusion, the system that represents the separately excited DC Motor is stable.

II.4 DC Motor parameters identification

As mentioned previously, the DC motor used in this project is a separately excited motor, thus, the DC motor parameters stand for finding the values of R_a, L_a, K_g, J and B . However, the value of R_f and L_f are useless since the field flux and current are constant. To find those constants, numerous steps are to be followed. Those steps are detailed in the following sections.

II.4.1 Identifying R_a and L_a :

a) DC test:

The DC test is done to identify the value of the armature resistance, the procedure is as follow:

1. Injecting many values of DC voltage to the armature ($V_{injected}$).
2. Motor must be at standstill (i.e. $\omega_m = 0$ and $e_a = 0$).
3. Measuring the equivalent value of the current corresponding to each value of the DC voltage ($I_{measured}$).
4. Drawing the graph $V_{injected}$ Vs $I_{measured}$.
5. Calculating the slope ($\frac{\Delta V_{injected}}{\Delta I_{measured}}$) of the drawn graph. That slope represents the armature resistance.

Table II-1 below represents the data gathered after a DC test on the used DC motor in this project.

Table II-1. DC test values.

$V_{injected}(V)$	0	10	20
$I_{measured}(A)$	0	4.5	8.5

The graph $V_{injected}$ Vs $I_{measured}$ is illustrated in figure II-2.

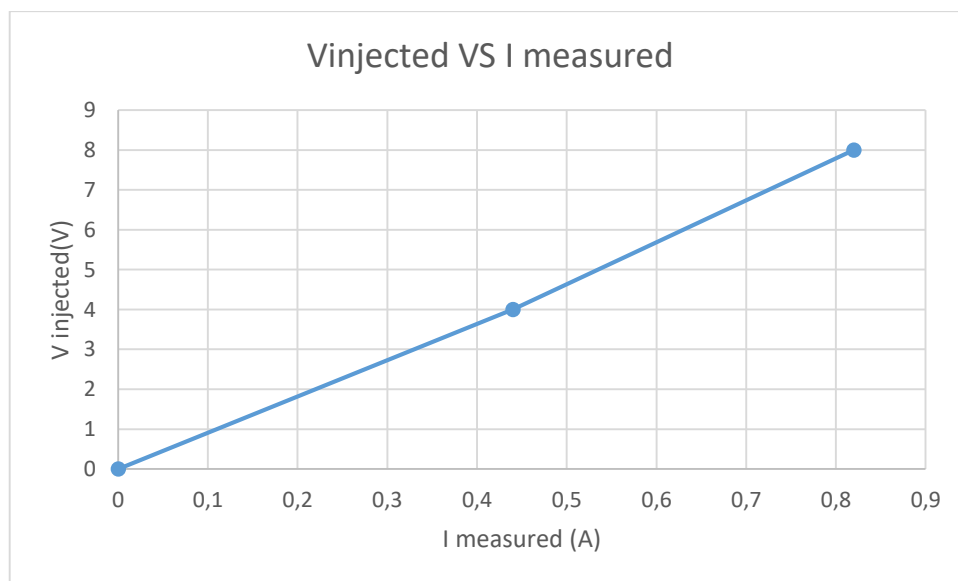


Figure II-2. the injected voltage versus the measured current graph

As expected the graph is a linear function so its slope is calculated such as:

$$\text{Slope} = \frac{\Delta V_{\text{injected}}}{\Delta I_{\text{measured}}} = \frac{20-10}{8.5-4.5} = 4.5$$

Thus, the value of R_a is equal to 4.5 Ω .

b) AC test:

The AC test is done to identify the value of the armature inductance, the procedure is as follow:

1. Injecting many values of AC voltage to the armature ($V_{ac\text{injected}}$).
2. Motor must be at standstill (i.e. $\omega_m = 0$ and $e_a = 0$).
3. Measuring the equivalent value of the current corresponding to each value of voltage ($I_{ac\text{measured}}$).
4. Drawing the graph $V_{ac\text{injected}}$ Vs $I_{ac\text{measured}}$.
5. Calculating the slope ($\frac{\Delta V_{ac\text{injected}}}{\Delta I_{ac\text{measured}}}$) of the drawn graph. That slope represents the magnitude of armature impedance Z_a .
6. Since the magnitude of Z_a is calculated as:

$$|Z_a| = \sqrt{R_a^2 + X_{L_a}^2}$$

Where:

- X_{L_a} is the reactance of the armature.

Thus:

$$X_{L_a} = \sqrt{|Z_a|^2 - R_a^2} = 2\pi f L_a$$

Where: - f is the frequency while measuring i.e. 50 Hz

Hence, the value of the armature inductance is: $L_a = \frac{\sqrt{|Z_a|^2 - R_a^2}}{2\pi f}$

Table II-2 represents the data gathered after an AC test on the DC motor.

Table II-2. AC test values

$V_{ac\text{injected}}$	0	4	8	10
$I_{ac\text{injected}}$	0	0.44	0.82	1.1

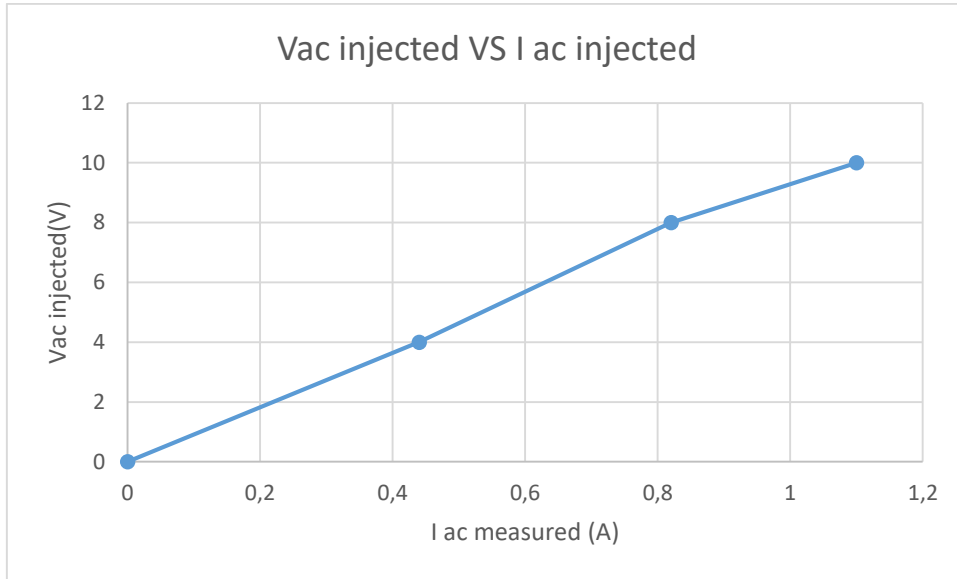


Figure II-3. The AC injected voltage versus the AC measured current

The graph $V_{ac_{injected}}$ Vs $I_{ac_{measured}}$ is illustrated in figure II-3. As expected the graph is approximately a linear function so its slope is calculated such as:

$$\text{Slope} = \frac{\Delta V_{ac_{injected}}}{\Delta I_{ac_{injected}}} = \frac{8-0}{0.82-0} = 9.756 \, \Omega$$

Using the equation of L_a shown in step 6, thus, L_a is equal to 0.0311 H.

II.4.2 Identifying K_g :

Taking in consideration the equation (II.4), it can be noticed that the back emf is directly proportional to the developed mechanical speed, thus, the steps to follow to find the approximated value of the motor constant are as the following:

1. Injecting many values of DC voltage to the armature without making the motor standstill (i.e. the motor must be running).
2. Measuring the output voltage through the motor (i.e. e_a).
3. Recording the equivalent values of the developed mechanical speed ω_m using a tachometer for the different values of e_a
4. Drawing the graph e_a vs ω_m , the graph should be a straight line passing through the origin.
5. Calculating the slope, this slope represents the coefficient of proportionality, hence, the slope is K_g .

Table II-3 represents the data gathered during the experiment of identifying K_g .

Table II-3. Back emf and their corresponding motor mechanical speed data

e_a	0	40	80	120	160	200
ω_m	0	185	357	565	758	955

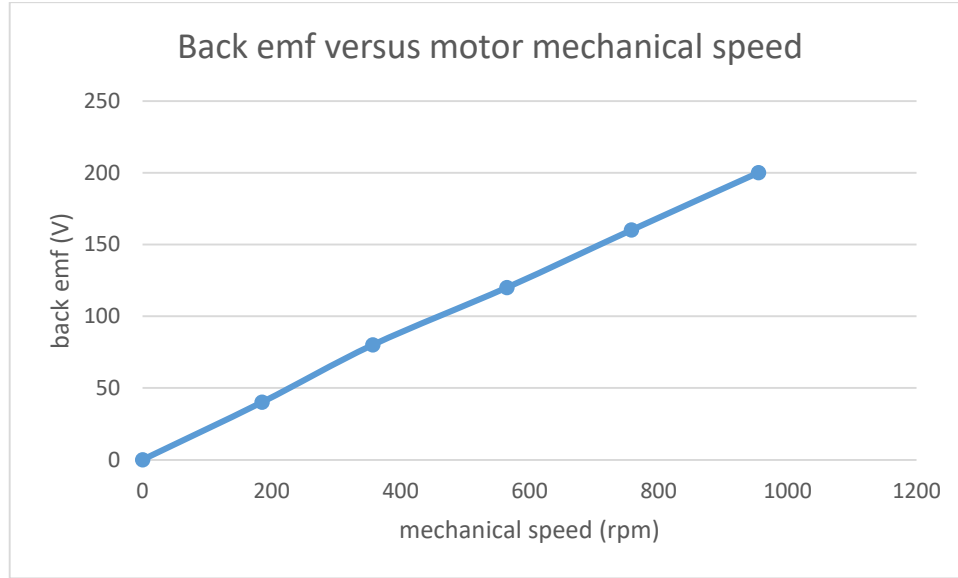


Figure II-4. Back emf versus mechanical speed graph

The graph e_a vs ω_m is illustrated in figure II-4. As expected the graph is approximately a straight line passing through the origin, so its slope is:

$$\text{Slope} = \frac{\Delta e_a}{\Delta \omega_m} = \frac{160-120}{758-565} = 0.2073 \text{ V/rpm}$$

Thus, the approximated value of K_g is 0.2073 V/rpm.

The value of K_g could be converted into V/rad/s, hence:

$$K_g = 0.2073 \text{ V/rpm} = 1.980 \text{ V/rad/s}$$

II.4.3 Identifying B:

Identifying the value the viscous friction requires many steps which are summarized as follow:

1. Turning on the DC motor without a load (i.e. $T_L = 0$ Nm).
2. Varying the values of the armature current by varying the injected DC voltage to the armature.

3. Waiting for the speed to stabilize and reaching its steady state value, thus, recording those corresponding values (I_a vs ω_m)
4. Hence, equation (II.2) could be write as follow:

$$T_e = B\omega_m \quad (\text{II.12})$$

Because:

- $T_L = 0 \text{ Nm}$
- ω_m is constant, thus, $\frac{d\omega_m}{dt} = 0$

Now, replacing (2.3) in (2.13): $K_g I_a = B\omega_m$

Finally,

$$B = K_g \frac{I_a}{\omega_m} \quad (\text{II.13})$$

Those steps were done, and the corresponding reading of the speed for a value of $I_a = 0.1 \text{ A}$ is $\omega_m = 170 \text{ rpm} = 17.802 \text{ rad/s}$

Hence, the value of B is calculated using the formula (II.13) and is equal to 0.01112 Nm/rad/s .

II.4.4 Identifying J:

To identify the value of J, many steps are to be followed:

1. Solving the differential equation (II.2) with respect to time, the solution is:

$$\omega_m(t) = \omega_{m0} e^{-\frac{t}{\tau}}$$

Where:

- ω_{m0} represents the maximum mechanical speed.
 - t is the time (s).
 - τ is time mechanical motor time constant and is equal to $\frac{J}{B}$
2. Fixing a value of mechanical speed that does not exceed the rated value.
 3. Recording this value, then turning off the DC motor.
 4. Recording the time needed to reach the half of the fixed value in step 2.
 5. Calculating the value of τ .
 6. Finally, computing the value of J .

The fixed value of the speed in the used DC motor during the experiment was set to $\omega_m = 1000$ rpm.

The time needed to reach the half of this value (i.e. 500 rpm) was 10.21 s.

Thus: $\tau = \frac{10.21}{\ln(2)} = 14.73$ s

Therefore, the moment of inertia is: $J = \tau B = 0.1638 \text{ kg}^2 \text{ m}^2 / \text{s}^2$

To summarize, table II-4 gives the obtained parameters that could be considered as a nameplate for the used DC motor.

Table II-4. DC Motor parameters

Rated Power (w)	2200
Rated Voltage (V)	220
Armature resistance (Ω)	4.5
Armature inductance (H)	0.0311
Motor constant ($V/\text{rad/s}$)	1.980
Viscous friction (Nm/rad/s)	0.01112
Moment of inertia ($\text{kg}^2 \text{ m}^2 / \text{s}^2$)	0.1638

DC motors are exceptionally eminent in various applications where speed is the foremost aspect such as industrial applications, robot manipulators and home appliances.

In this project, the main objective is to control the speed of the used DC Motor by controlling the input armature voltage.

III.1 Speed and torque characteristics and control:

In steady state operation and since the current will stabilize, the equation (II.1) becomes:

$$V_a = R_a I_a + e_a \quad (\text{III.1})$$

Replacing (II.4) in (III.1) and rearranging it:

$$\omega_m = \frac{V_a}{K_g} - \frac{R_a I_a}{K_g} \quad (\text{III.2})$$

From equation (II.3) the expression of the armature current with respect to the induced torque is:

$$I_a = \frac{T_e}{K_g} \quad (\text{III.3})$$

Thus, replacing (III.3) in (III.2), the expression of the motor mechanical speed with respect to the induced torque is as follow:

$$\omega_m = \frac{V_a}{K_g} - \frac{R_a T_e}{K_g^2} \quad (\text{III.4})$$

The equation (III.4) has a form of a straight line, its equation has a form of $y = ax + b$;

Where:

- y represents the output function ω_m
- a is the tangent and is equal to $-\frac{R_a}{K_g^2}$
- x is the variable T_e
- b is the intersection between the graph and the (oy) axis and is equal to $\frac{V_a}{K_g}$

From equation (III.4) it can be noticed that the mechanical speed of a separately excited DC Motor is inversely proportional to the torque induced. When the induced torque increases, the mechanical speed decreases.

From the equation (III.4), three possible methods for speed control can be derived, those techniques are as follow:

- a) Armature resistance R_a control
- b) Field flux ϕ control¹
- c) Armature voltage V_a control

Those techniques are discussed in details in the following sections.

III.1.1 Armature resistance control

From equation (III.4), it can be noticed that the slope of the straight line that represents the graph of the mechanical speed with respect to the induced torque depends on the value of the armature resistance, and since the value of K_g is kept constant, thus varying the value of R_a is varying the value of the slope and thus the value of ω_m . The more the value of R_a is increased the more the slope decreases. Figure III-1 illustrates the impact of varying the value of R_a on the speed.

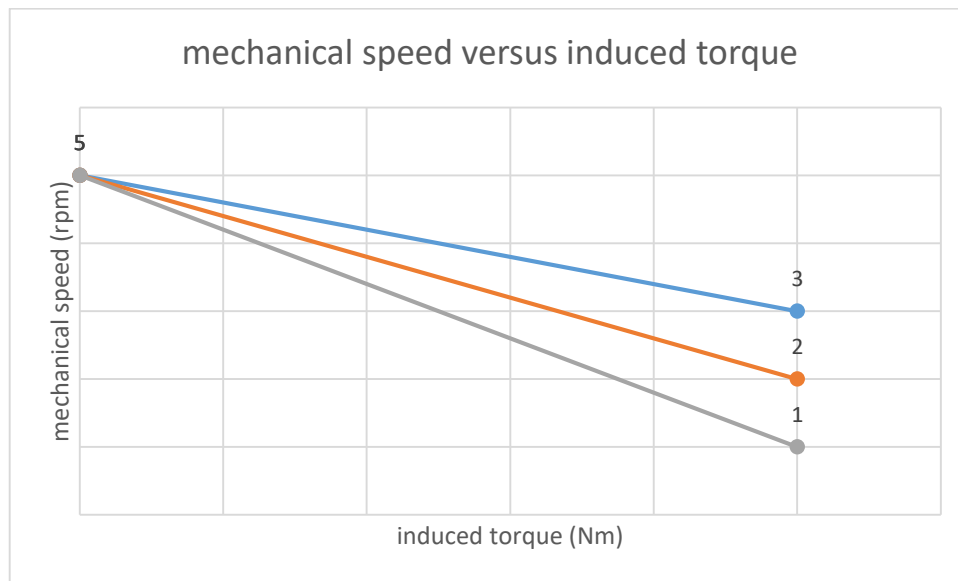


Figure III-1. The impact of varying the armature resistance on the mechanical speed.

Comments:

- The blue graph represents the equation (III.4) using an initial random value R_{a1}
- The orange graph represents the equation (III.4) with an increase in the value of the armature resistance R_{a2} such that $R_{a2} > R_{a1}$

¹ Since $K_g = K\phi$ and K is constant, thus varying K_g is varying ϕ .

- The grey graph represents the equation (III.4) with an increase in the value of the armature resistance R_{a3} such that $R_{a3} > R_{a2} > R_{a1}$
- The intersection between the 3 graphs and the y-axis which represents the initial mechanical speed is not affected by the change on the value of R_a because this intersection is independent from the armature value and is equal to $\frac{V_a}{K_g}$ where the values of V_a and K_g are kept constant.

Advantages of the armature resistance control:

- Simple control process.

Disadvantage of the armature resistance control:

- Increasing power losses due to the increasing of the armature resistance ($P_{losses} = R_a I_a^2$)
- Reducing the power efficiency.
- Armature resistance control is restricted to keep the speed below the normal speed of the motor and increase in the speed above normal level is not possible by this method.
- Rarely used.
- External parameters could interfere with the value of the armature resistance (ex: temperature).

III.1.2 Field flux ϕ control:

As seen previously one of the 3 methods to control the mechanical speed is controlling the flux ϕ . However, since the used DC motor is a separately excited type, thus, to vary the value of ϕ the value of the field voltage V_f need to be varied.

This method of controlling is not used in permanent magnet DC Motor because the flux is always constant.

The more the flux is increased the more the slope is increased to zero, the less the initial value of the mechanical speed ω_{m0} is, because, the slope is equal to $-\frac{R_a}{K_g^2} = -\frac{R_a}{(K\phi)^2}$ so, the slope increases rapidly to zero and the initial mechanical speed will decrease too since $\omega_{m0} = \frac{V_a}{K\phi}$.

Figure III-2 shows the effect of increasing the value of the flux.

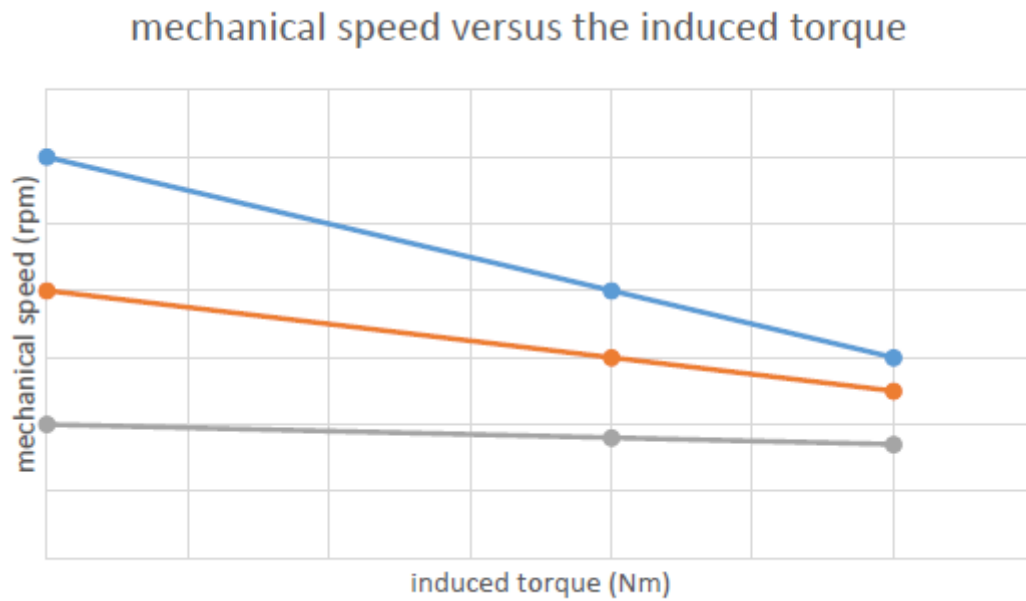


Figure III-2. The effect of increasing the flux on the mechanical speed

Comments:

- As said previously the more the flux is increased the more the speed is decreases.
- The blue graph represents the graph of the speed versus the torque with an initial value of ϕ_0
- The orange graph represents the graph of the speed versus the torque with an increase in the previous value of the flux, this value if called ϕ_1 such that $\phi_1 > \phi_0$.
- The grey graph represents the graph of the speed versus the torque with an increase in the previous value of the flux, this value if called ϕ_2 such that $\phi_2 > \phi_1 > \phi_0$.
- The initial value of the speed also decreases with an increase in the flux field as shown in the figure III-2 shown above.

As a conclusion, for a use purpose if the mechanical speed needs to be increased then the field flux needs to be reduced.

Advantages of field flux control:

- Reversing the speed is simple, all it needs is reversing the voltage field and thus the field flux is reversed, hence the speed is reversed also.
- The control process is simple and used generally for speed above the base speed.

Disadvantages of field flux control:

- Varying the flux is impossible for permanent magnet DC motor.

III.1.3 Armature voltage control:

As seen in equation (III.4), the mechanical speed is related also to the armature voltage V_a and it represents the y axis intersection (the initial mechanical speed ω_{m0}). However, the slope remains constant during the variation of the armature voltage because it is independent of the armature voltage.

The field voltage need to be maintained constant to maintain the field flux constant too. If the armature voltage is increased, thus, ω_{m0} is increased also, and vice versa.

Figure III-3 shown below illustrates the impact of increasing the value of the armature voltage.

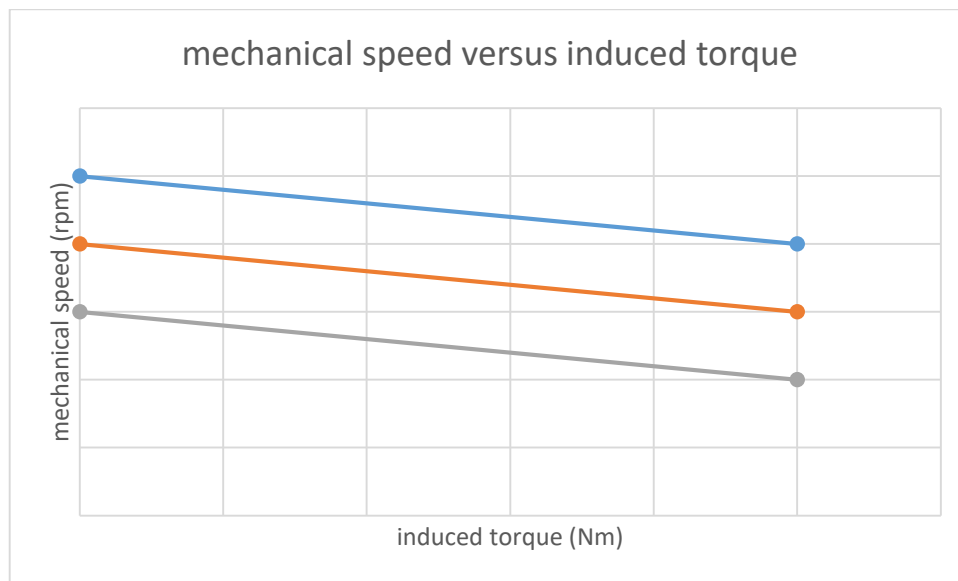


Figure III-3. The impact of increasing the armature voltage on the mechanical speed.

Comments:

- The grey graph represents the mechanical speed versus the induced torque with an initial value of the armature voltage V_{a0} .
- The orange graph represents also the mechanical speed versus the induced torque but with an increase in the value of the armature voltage V_{a1} such that: $V_{a1} > V_{a0}$
- The blue graph represents also the mechanical speed versus the induced torque with another increase in the armature voltage V_{a2} such that: $V_{a2} > V_{a1} > V_{a0}$.

As said previously, figure III-3 confirms that the more the armature voltage is the more the mechanical speed is.

Advantages of armature voltage control:

- Speed is controlled from 0 to the base speed.
- The speed can be limited by fixing the value of the armature voltage and thus avoiding insulating damages².

Disadvantages of armature voltage control:

- Cannot be used to control the speed beyond and base speed.

Remark:

The previous control techniques can be combined to control the mechanical speed above and beyond the base speed. One of the most used combined control technique is armature and field control.

In this project, the armature voltage control technique will be used to control the speed of the used separately excited DC motor.

III.2 Operation modes:

Operation modes of a DC motor depend on how the motor runs, there are 4 modes of operation, and those modes are:

- Forward motoring:** forward motoring is one of the most used mode of operation where the speed and the torque are both positive. This mode of operation consists of converting electrical energy into mechanical energy. It is generally referred as Quadrant 1 (Q1) operation.
- Forward breaking:** forward breaking is a mode of operation where the DC motor works as a generator, thus, the motor will convert mechanical energy into electrical energy. It is generally referred as Quadrant 2 (Q2) operation. The speed is positive, however, the torque is negative.
- Reverse motoring:** reverse motoring is a type of motoring where the DC motor works as a motor but in the reverse direction of the forward motoring, both the speed and the torque are negative. This mode of operation is referred as Quadrant 3 (Q3) operation.

² Insulating damages are failures that are caused by the low insulating resistance which causes the non-isolation between the conductors or motor windings.

d) Reverse braking: reverse braking mode is referred as 4th Quadrant operation (Q4). The speed is negative where the torque is positive, thus, the motor works as a generator.

Operation modes are summarized in the figure III-4.

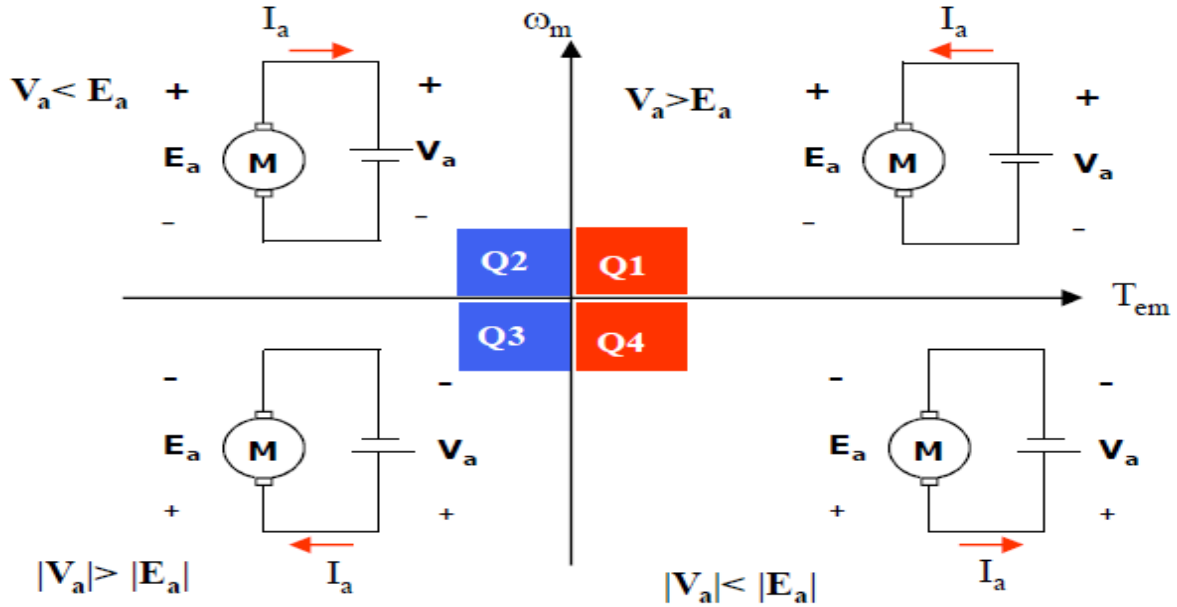


Figure III-4. The DC motor four quadrant modes[3].

III.3 Open loop control:

As said previously, the used control technique in this project is the armature voltage control. Hence, controlling this voltage is the main purpose of this chapter.

The process of controlling the armature voltage is called the open loop control, while the process of controlling the speed of the DC motor is called the closed loop control (it will be seen in the next part).

The armature of the DC motor is fed from a DC source V_a . This armature voltage is controlled using two types of electronic devices:

- DC choppers.
- Controlled rectifiers.

In this project only the DC chopper is used for controlling the armature voltage.

III.3.1 DC choppers:

In electronics, a chopper circuit is used to refer to numerous types of electronic switching devices and circuits used in power control and signal applications. A chopper is a device that converts fixed DC input to a variable DC output voltage directly. Essentially, a chopper is an electronic switch that is used to interrupt one signal under the control of another [2]. Chopper circuits are used in multiple applications, including:

- Switched mode power supplies, including DC to DC converters.
- Speed controllers for DC motors.

Since the used motor in this project is a DC motor, so it may be fed from a DC source, a battery or a PV cells³. In this project the DC motor is fed from a DC source. Thus, a DC chopper is used to regulate and control the amount of DC output feeding the DC motor, hence, controlling the armature voltage and the speed which has a direct relationship with the armature voltage as seen previously. Figure III-5 shows the simplest scheme of a DC to DC chopper.

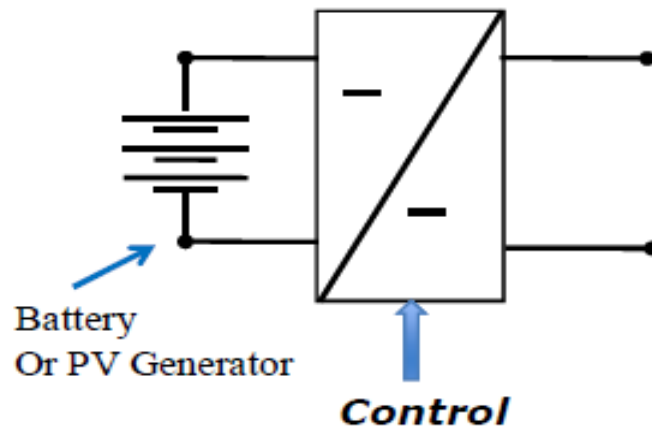


Figure III-5. A DC to DC Scheme of a DC chopper[3].

In this project the Pulse width modulation (PWM) will be used as the control of the DC chopper (will be discussed in the next session).

III.3.1.1 Principle of operation of a DC chopper:

The principle of operation of the DC chopper is that A DC source is directly connected to the DC motor through switches and freewheeling diodes, and those switches are controlled via PWM.

³PV cells are photovoltaic cells used in solar energy to produce a DC power.

The chopper is ON for a time t_{ON} and OFF for a time t_{OFF} . The switching frequency is given by the following formula:

$$f_c = \frac{1}{t_{ON} + t_{OFF}} = \frac{1}{T} \quad (III.5)$$

Where:

- T is the time period in seconds.

Assuming that the switches are ideal, thus:

$$V_a = \frac{1}{T} \int_0^{t_{ON}} V_s dt = \frac{t_{ON} V_s}{T} \quad (III.6)$$

Where:

- The duty cycle is given by:

$$d = \frac{t_{ON}}{T} \quad (III.7)$$

Replacing (III.7) in (III.6), therefore:

$$V_a = d V_s \quad (III.8)$$

Figure III-6 shown below, shows how the DC motor is connected through a DC chopper.

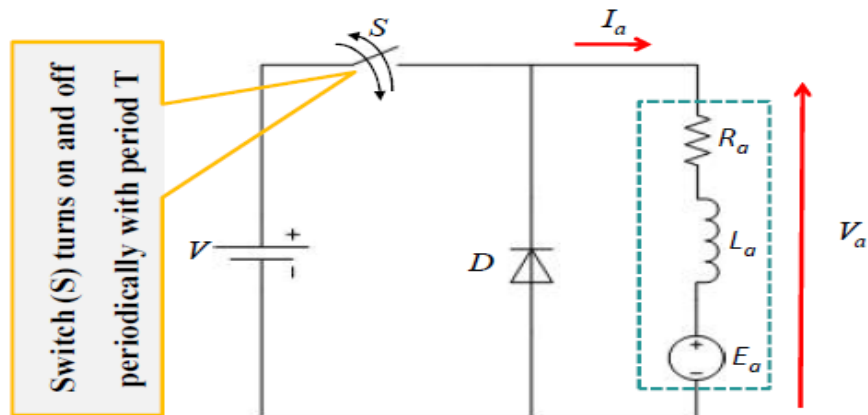


Figure III-6. Equivalent circuit of a DC motor connected to a DC chopper [3].

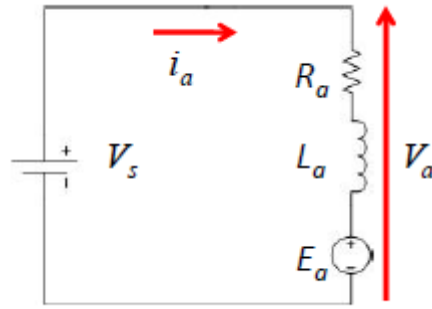


Figure III-7. The equivalent circuit when the switch S is closed[3].

The previous circuit shown in figure III-6 has two different working principle, thus:

- If the switch S is closed: ($0 \leq t \leq t_{ON}$)

Figure III-7 illustrates the working principle of the DC motor when the switch S is closed.

In figure III-7, it can be noticed that:

- $V_s = V_a$
- I_a flows to the motor.
- I_a increases.

- If the switch S is off: ($t_{ON} \leq t \leq T$)

Figure III-8 illustrates the working principle of the DC motor when the switch S is opened. It can be noticed that:

- $V_s = 0$
- I_a freewheels through diode.
- I_a decreases.

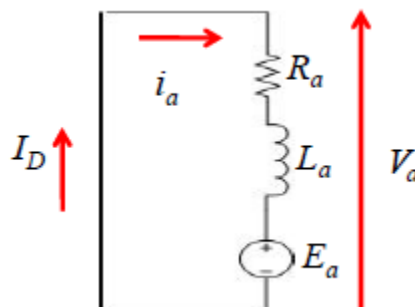


Figure III-8. The equivalent circuit when the switch S is open [3].

The value of the armature current I_a is then directly related to the duty cycle of the DC chopper, such that:

$$I_a = \frac{dV_s - K_g \omega_m}{R_a} \quad (\text{III.9})$$

Thus, the developed torque is also directly related to the duty cycle as seen in equation (II.9).

III.3.1.2 Advantage of using DC chopper

- Controlled rectifier introduces harmonics to supply currents and voltages, which cause heating and torque pulsations in motor.
- Avoiding more harmonics in the primary current which contribute to pollute the network in case of the use of a rectifier.
- Employ pulse-width modulated (PWM) rectifiers using GTOs, IGBTs to improve power factor, overcome the effect of low order harmonics and subsequently reduce pulsations and derating.

III.3.1.3 Controlling the DC chopper

The control of the DC chopper (i.e. the control of the switches S) is done in this project using the PWM.

Pulse width modulation (PWM) is a method of reducing the average power delivered by an electrical signal, by effectively chopping it up into discrete parts. The average value of voltage (and current) fed to the load is controlled by turning the switch between supply and load on and off at a fast rate. The longer the switch is on compared to the off periods, the higher the total power supplied to the load [4].

III.4 Closed loop control:

In the industry, most drive systems operate as a closed loop with feedback systems. The torque-speed characteristics of the DC-motor show that for constant armature voltage, if the load torque is increased the speed will change. However, because most drive systems used in the industry require maintaining constant speed; a closed loop control system must be introduced.

The block diagram of such a system is shown in figure III-9.

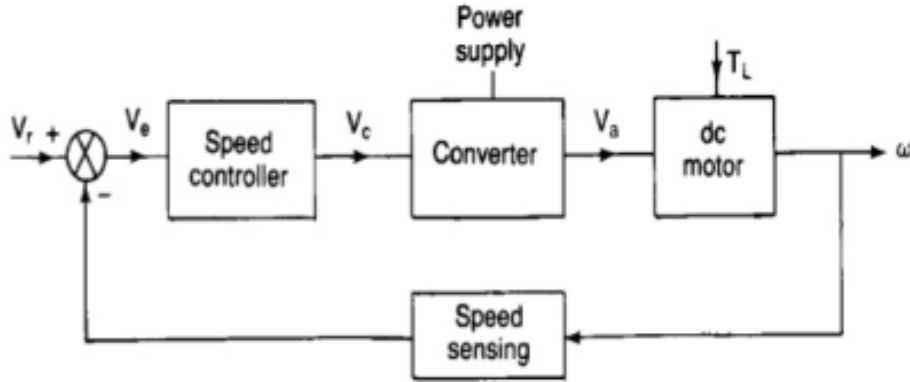


Figure III-9. Block diagram of a closed- loop speed control system.

If the motor speed decreases due to an increase in the load torque, the measured speed at the motor shaft is fed back and compared with a reference speed. The difference speed error is applied to the speed controller to generate a control voltage V_c which controls the power converter and produces the desired armature voltage V_a . The armature voltage controls the speed of the motor and thus the speed of the motor can be maintained for any variations in the load torque.

A closed loop system has the advantages of greater accuracy, improved dynamic response and reduced effects of disturbances without any major deviations. When the drive needs to meet some performance requirements, the closed-loop system is necessary.

III.5 Separately excited DC motor drive:

The separate excitation of the DC motor makes the speed and torque control relatively simple. In most applications, the excitation voltage is kept constant and the armature voltage is controlled by a closed loop system, the system may have some protective features, such as current limiting. For the assessment of the dynamic response of the drive system the transfer function of the motor and the control elements are derived.

III.5.1 Motor Transfer Function

Considering a separately excited DC motor with armature voltage control. The electrical equation is:

$$V_a = E_a + R_a I_a + L_a \frac{dI_a}{dt} \quad (\text{III.10})$$

Where $E_a = K_g \omega_m$.

The mechanical equation is:

$$T_e = J \frac{dw_m}{dt} + Bw_m + T_L \quad (\text{III.11})$$

Where

$$T_e = K_g I_a \quad (\text{III.12})$$

Taking Laplace transform, the above equations can be written as:

$$V_a(s) = K_g w_m(s) + (R_a + L_a s) I_a(s) \quad (\text{III.13})$$

$$K_g I_a(s) = (Js + B) w_m(s) + T_L(s) \quad (\text{III.14})$$

Thus, from equation (III.13):

$$I_a(s) = \frac{V_a(s) - K_g w_m(s)}{R_a + L_a s} = \frac{(V_a(s) - K_g w_m(s))^{1/R_a}}{1 + sT_a} \quad (\text{III.15})$$

Where

$$T_a = \frac{L_a}{R_a} \text{ is the electrical time constant of the motor.}$$

From equation (III.14):

$$w_m(s) = \frac{K_g I_a(s) - T_L(s)}{Js + B} = \frac{(K_g I_a(s) - T_L(s))^{1/B}}{1 + sT_m} \quad (\text{III.16})$$

Where

$$T_m = \frac{J}{B} \text{ is the mechanical time constant of the motor.}$$

Equations (III.15) and (III.16) are used to construct the block diagram of figure III-10.

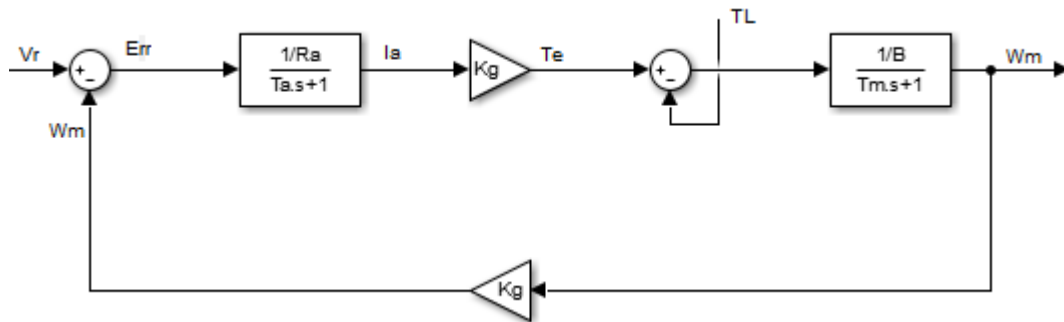


Figure III-10. Separately excited DC motor block diagram

Where:

- $T_a = \frac{L_a}{R_a}$ is the electrical time constant of the motor.
- $T_m = \frac{J}{B}$ is the mechanical time constant of the motor.

From the block diagram, if the load torque term is neglected:

$$\frac{w_m(s)}{V_a(s)} = \frac{\frac{K_g}{R_a B(1+sT_a)(1+ST_m)}}{1 + \frac{K_g^2}{R_a B(1+sT_a)(1+ST_m)}} \quad (\text{III.17})$$

$$\frac{w_m(s)}{V_a(s)} = \frac{K_g}{K_g^2 + R_a B(1+sT_a)(1+ST_m)} \quad (\text{III.18})$$

Since the armature controlled operation is used, the armature inductance L_a is small and can be neglected. Therefore, the expression simplifies to:

$$\frac{w_m(s)}{V_a(s)} = \frac{K_g}{K_g^2 + R_a B + sR_a B T_m} \quad (\text{III.19})$$

$$\frac{w_m(s)}{V_a(s)} = \frac{K_m}{1+sT_{m1}} \quad (\text{III.20})$$

Where:

$$T_{m1} = \frac{R_a B T_m}{K_g^2 + R_a B} \quad (\text{III.21})$$

$$K_m = \frac{K_g}{K_g^2 + R_a B} \quad (\text{III.22})$$

In addition, from the block diagram, we have:

$$\frac{w(s)}{I_a(s)} = \frac{K_g/B}{1+sT_m} = \frac{K_{m2}}{1+sT_m} \quad (\text{III.23})$$

Hence, from equations (III.20) and (III.23):

$$\frac{I_a(s)}{V_a(s)} = \frac{K_m B(1+sT_m)}{K_g(1+sT_{m1})} = \frac{K_{m1}(1+sT_m)}{1+sT_{m1}} \quad (\text{III.24})$$

Where,

$$K_{m1} = \frac{B}{K_g^2 + R_a B} \quad (\text{III.25})$$

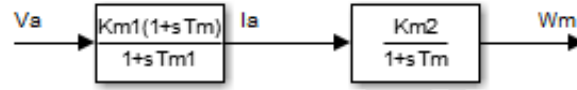


Figure III-11. Simplified block diagram for DC motor.

Thus, the motor can be represented by two blocks in order to simplify further analysis as shown in figure III-11.

III.5.2 Power converter transfer function:

A chopper controls the applied armature voltage. The equation describing the chopper is given by:

$$V_{out} = DV_{DC} \quad (III.26)$$

Where D is the duty cycle of the PWM signal. The basic technique to generate PWM signal is shown in figure III-13 bellow.

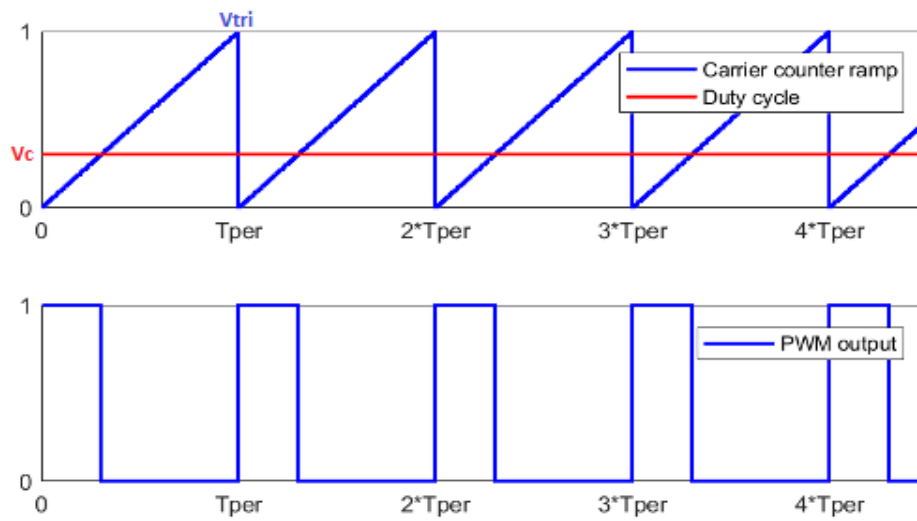


Figure III-12. PWM ganeration

From the above figure, we can notice that the control signal V_c is compared with a carrier signal, if the control signal is less than the carrier the PWM output is set to high, otherwise is low. Therefore, the duty cycle can be expressed as:

$$D = \frac{V_c}{V_{tri}} \quad (III.27)$$

Where,

- V_{tri} is the maximum of the carrier signal.

- V_c is the control signal.

Thus, substituting equation (III.27) in equation (III.26):

$$V_{out} = \frac{V_{DC}}{V_{tri}} V_c \quad (III.28)$$

$$V_{out} = K_c V_c \quad (III.29)$$

Hence, the converter gain is:

$$K_c = \frac{V_{DC}}{V_{tri}} \quad (III.30)$$

III.5.3 The speed controller:

A tacho-generator is attached to the motor shaft so that a speed signal can be fed back and the error signal V_e is used by the controller to generate a control signal V_c . The speed controller is of a proportional integral type. The PI transfer function is represented as

$$G_s(s) = K_s \frac{(1+sT_s)}{sT_s} \quad (III.31)$$

III.6 Closed-loop speed control

After identifying all the elements transfer functions, the speed control loop is constructed and is shown in figure III-13 below.

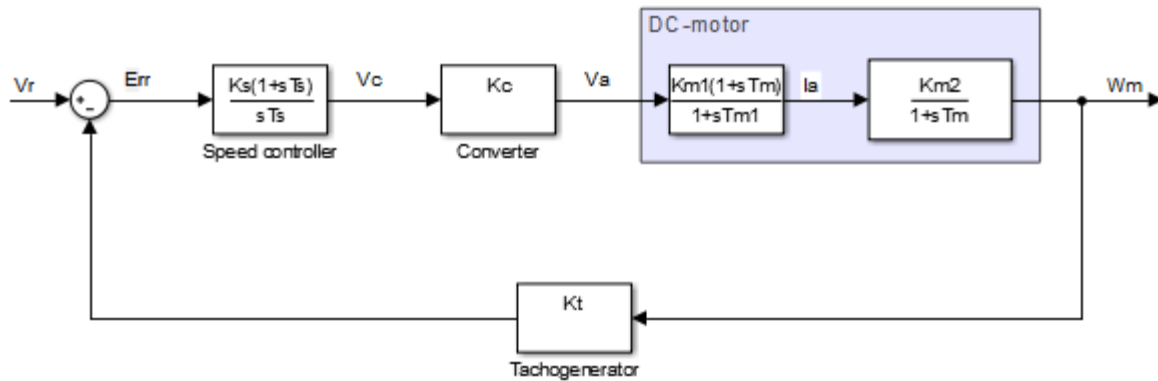


Figure III-13. Speed control-loop block diagram.

The closed-loop transfer function of the block diagram shown in figure III-13 is as follow:

$$\frac{w_m(s)}{V_r(s)} = \frac{G(s)}{1+G(s)H(s)} \quad (III.32)$$

Where:

- $G(s) = \frac{K_s K_c K_{m1} K_{m2} (1+sT_s)}{sT_s(1+sT_{m1})}$
- $H(s) = K_t$

With: K_t is the gain of the tacho-generator.

Hence,

$$\frac{w_m(s)}{V_r(s)} = \frac{K_s K_c K_{m1} K_{m2} (1+sT_s)}{sT_s(1+sT_{m1}) + K_t K_s K_c K_{m1} K_{m2} (1+sT_s)} \quad (\text{III.33})$$

Setting: $T_s = T_{m1}$

Therefore,

$$\frac{\omega_m(s)}{V_r(s)} = \frac{K_s K_c K_{m1} K_{m2}}{sT_{m1} + K_t K_s K_c K_{m1} K_{m2}} \quad (\text{III.34})$$

Equation (III.34) can be reduced to:

$$\frac{w_m(s)}{V_r(s)} = \frac{K_1}{1+ST_1} \quad (\text{III.35})$$

Where:

- $K_1 = \frac{1}{K_t}$
- $T_1 = \frac{T_{m1}}{K_t K_s K_c K_{m1} K_{m2}}$

Therefore,

$$\frac{I_a(s)}{V_r(s)} = \frac{w_m(s)}{V_r(s)} \frac{I_a(s)}{w_m(s)} = \frac{K_1}{1+ST_1} \frac{1+sT_m}{K_{m2}} = \frac{K_1(1+sT_m)}{K_{m2}(1+ST_1)} \quad (\text{III.36})$$

Thus, the current response to a step change in input V_r is:

$$I_a(s) = \frac{K_1 V_r (1+sT_m)}{K_{m2} s(1+sT_1)} \quad (\text{III.37})$$

Using partial fraction:

$$I_a(s) = \frac{A}{s} + \frac{B}{s(1+sT_1)}$$

Where:

- $A = \frac{K_1 V_r}{K_{m2}}$
- $B = \frac{K_1 V_r}{K_{m2}} (T_m - T_1)$

Hence,

$$I_a(s) = \frac{K_1 V_r}{K_{m2}} \left(1 + \frac{T_m - T_1}{T_1} \frac{1}{\frac{1}{T_1} + s} \right) \quad (\text{III.38})$$

Using inverse Laplace transform to find the time expression of the current in the time domain:

$$I_a(t) = \frac{K_1 V_r}{K_{m2}} \left(1 + \frac{T_m - T_1}{T_1} e^{-t/T_1} \right) \quad (\text{III.39})$$

From this equation, we can notice that a change in the reference input voltage V_r results in a large change in the armature current I_a which decays in time. From the standpoint of power converter rating and protection, this transient overcurrent is undesirable and may damage the solid-state devices used in the power converter.

III.7 The closed-loop current (torque) control

The previous analysis revealed that an increase in the reference voltage causes the armature current to increase drastically. Therefore, it is necessary to limit the current to some maximum allowable value. This cannot be obtained using the block diagram of figure III-13 where the power converter is controlled by the speed controller. Clamping the speed controller output will limit the motor armature voltage that will limit the speed but not the current. A current limit can be obtained by introducing a current control loop and using the speed controller output for the current reference as shown in figures III-14 and III-15

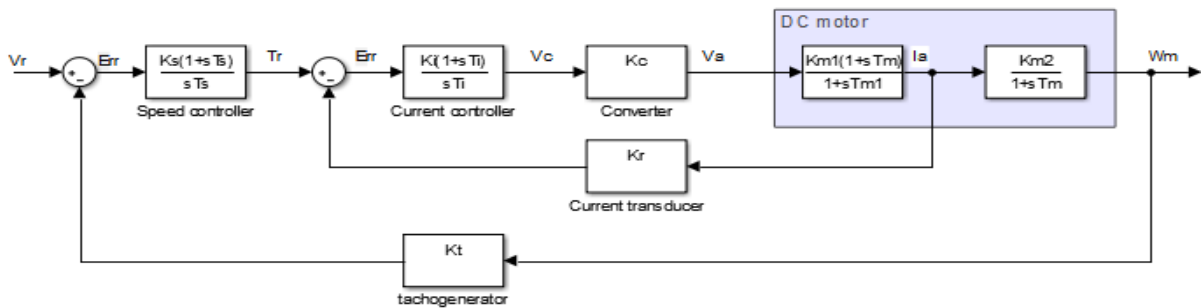


Figure III-14. Speed and current (torque) control block diagram.

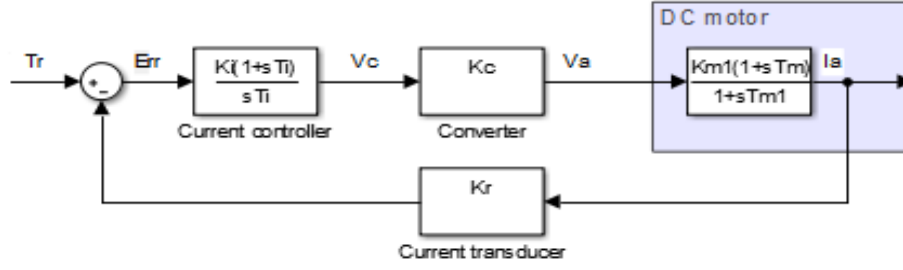


Figure III-15. Current (torque) control loop block diagram.

The closed loop transfer function of the block diagram of the current control shown in figure III-15 is:

$$\frac{I_a(s)}{T_r(s)} = \frac{\frac{K_i K_c K_{m1} (1+sT_i)(1+sT_m)}{sT_i(1+sT_{m1})}}{1 + \frac{K_i K_c K_{m1} K_r (1+sT_i)(1+sT_m)}{sT_i(1+sT_{m1})}} \quad (\text{III.40})$$

Where:

- K_r is current transducer gain.

Simplifying and rearranging the equation (III.34):

$$\frac{I_a(s)}{T_r(s)} = \frac{K_i K_c K_{m1} (1+sT_i)(1+sT_m)}{sT_i(1+sT_{m1}) + K_i K_c K_{m1} K_r (1+sT_i)(1+sT_m)} \quad (\text{III.41})$$

Setting: $T_i = T_{m1}$

$$\frac{I_a(s)}{T_r(s)} = \frac{K_i K_c K_{m1} (1+sT_m)}{K_i K_c K_{m1} K_r + s(T_{m1} + K_i K_c K_{m1} K_r T_m)} \quad (\text{III.42})$$

Since: $T_m > T_{m1}$ and $K_i K_c K_{m1} K_r \gg 1$

$$\frac{I_a(s)}{T_r(s)} = \frac{K_i K_c K_{m1} (1+sT_m)}{K_i K_c K_{m1} K_r + s(K_i K_c K_{m1} K_r T_m)} \quad (\text{III.43})$$

Finally,

$$\frac{I_a(s)}{T_r(s)} = \frac{1/K_r (1+sT_m)}{(1+sT_m)} = \frac{1}{K_r} = K_{ic} \quad (\text{III.44})$$

From the above equation, it can be notice that it is possible to limit the current to some safe value by clamping the speed controller output to a maximum value \hat{T}_r and this will limit the current to the maximum value: $\hat{I}_a = K_{ic} \hat{T}_r$.

Chapter IV: Simulation of the control system

For designing a control system, some of the design work can be performed by hand, but it is difficult to do the verification and the checking of the result or the simulation of the system's responses by hand. Therefore, it is necessary to introduce some tools such as MATLAB that can help to simulate the system and check the different responses before the implementation.

MATLAB is a sophisticated software tool. It is provided with SIMULINK, which is a block diagram environment for simulation and model-based design. It allows designing and simulating the system before the hardware implementation without having to write a code for the design.

IV.1 SIMULINK model of the control system:

The block diagram shown in figure IV-1 is implemented using SIMULINK in order to simulate the control system and to tune the PI controllers, so that the desired performance parameters can be attained.

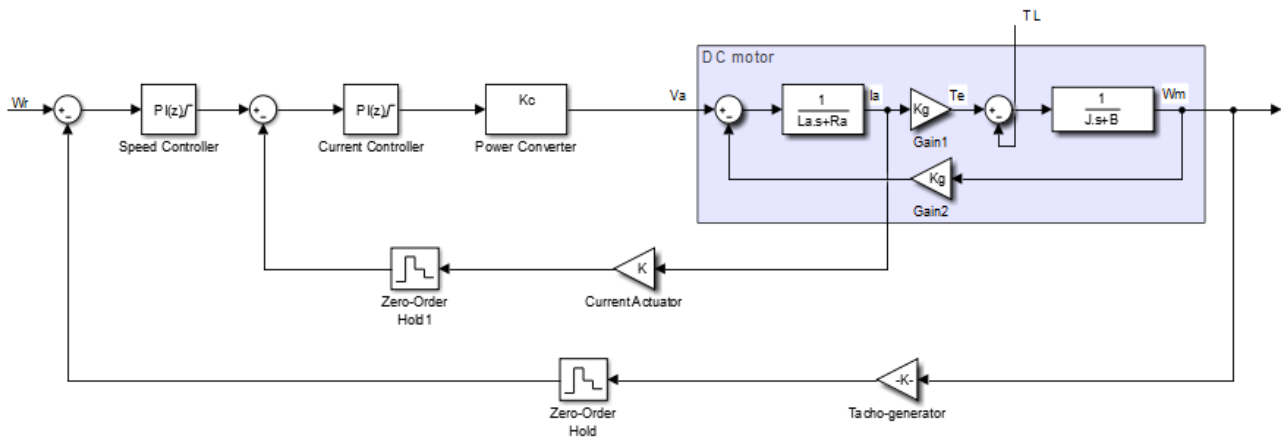


Figure IV-1. SIMULINK block diagram.

IV.2 The controller parameters tuning:

A control system has to meet certain conditions and specifications, which depends on the performance requirements. And the least condition that has to be satisfied for a control system is that the transient components should not go to infinity for any bounded input. This is the condition for absolute stability for a linear system.

In addition, for a control system insuring only stability is not sufficient, certain specifications have to be satisfied such as:

- a. Reducing the steady state error within an allowable limit in order to improve the system performance.
- b. Reducing the peak overshoot, in our case to avoid the transient over current, which is undesirable from the standpoint of protection and converter rating especially in the case of starting or a large change in the reference signal.

To attain these objectives, the exact values of the controller parameters K_p and K_I have to be chosen. The analytical method, Ziegler-Nichols, trial and error and software tools are methods used for controller tuning. A software tool named “PID tuner” which is provided with SIMULINK was used in this project.

IV.3 PID tuner:

Choosing the best set of PID controller parameters that guarantee the desired performance and meet the design requirements for a control system is a complex task. The conventional methods that are used for PID tuning are either manual or rule-based. These methods have serious limitations when it comes to support certain types of systems such as high order systems and unstable systems.

Consequently, “PID tuner tool” which is a software tool provided with SIMULINK is used for tuning the PID controller automatically to achieve the optimal system design and meet the design requirement.

The parameters of the PI controllers obtained using “PID tuner tool” as shown in the figures IV-2 and IV-3 bellow.

Controller Parameters	
	Tuned
P	9.2582
I	1.0802

Figure IV-2. PI speed controller parameters.

Controller Parameters	
	Tuned
P	0.31761
I	2.2235

Figure IV-3. PI current (torque) controller parameters.

IV.4 Simulation results:

The reference speed is set to 100 rpm then the speed vs time waveform is plotted.

Figure IV-4 below shows the plot w_r vs time.

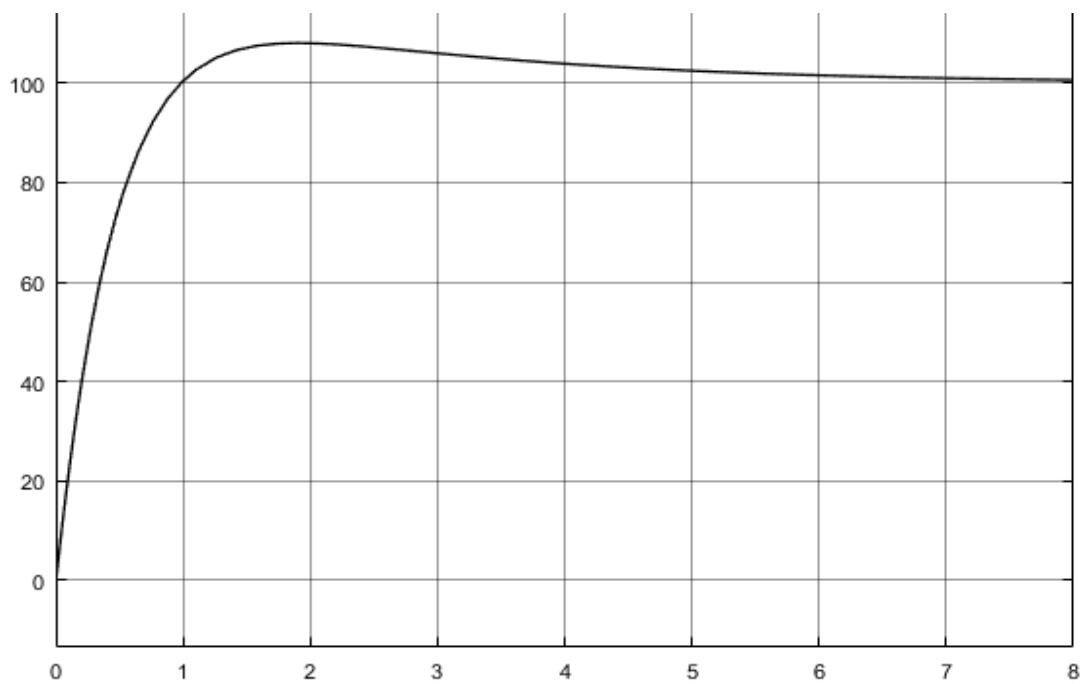


Figure IV-4 speed waveform with $w_r = 100$ rpm

Figure IV-5 shown in the next page shows the waveform plot of the armature current (A) vs time (s) with the motor at full load.

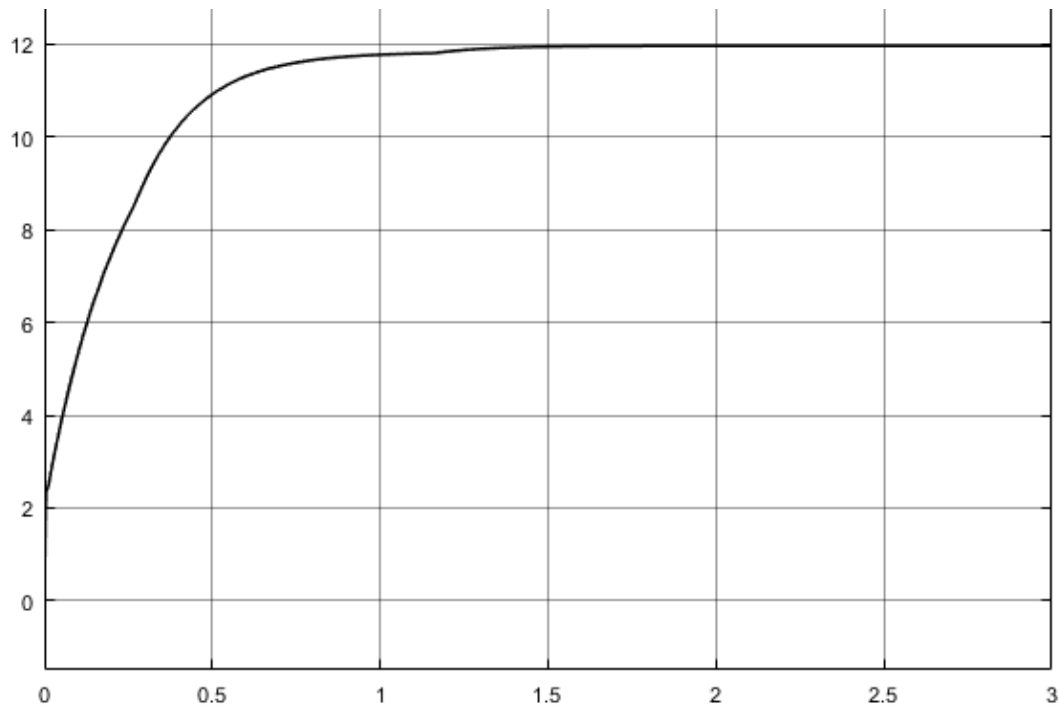


Figure IV-5. Armature current waveform at full load.

Figures mentioned above show that :

- The motors speed is being regulated and it is stabilized at a final value of 100 rpm.
- The armature current is controlled and does not increase drastically.
- The armature current increases slowly to produce the required torque.

Then, the reference speed is set to 600 rpm and then it is changed to 1200 rpm.

Figure IV-6 next page shows the speed waveform for a reference speed of 600 rpm then 1200 rpm.

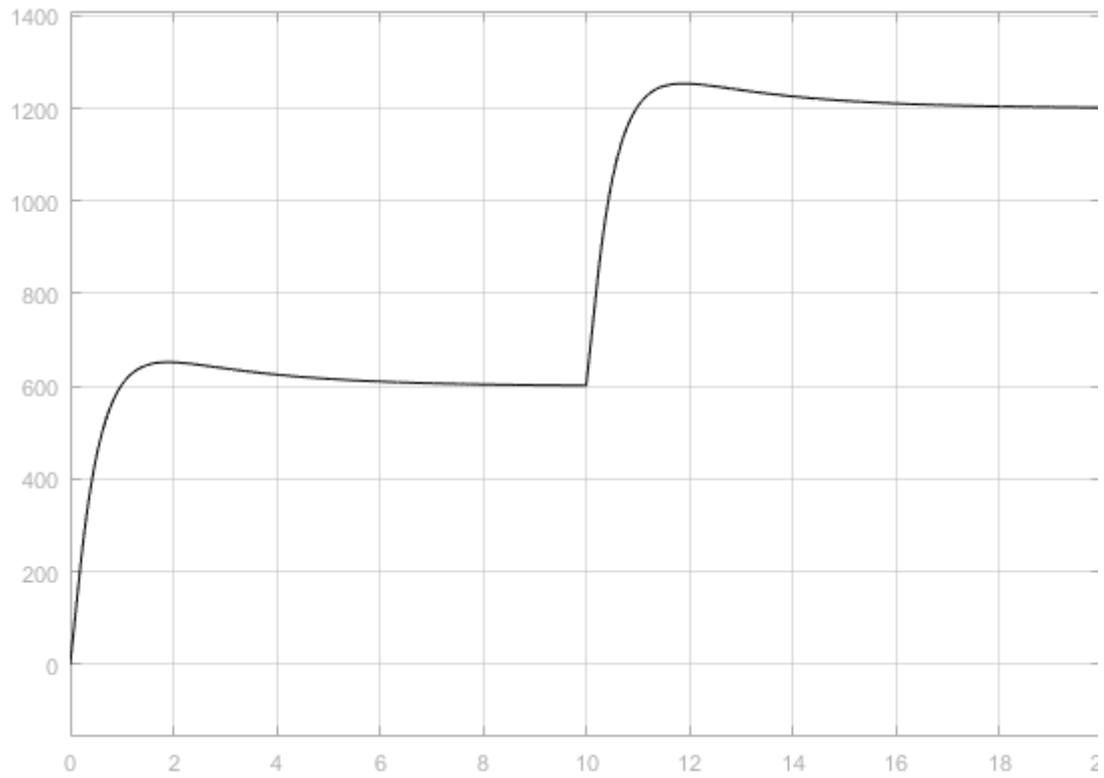


Figure IV-6 speed (rpm) vs time for $W_r=600$ rpm then $W_r=1200$ rpm

For the below figure, a load torque of 0 Nm is applied at the beginning and then it is changed to 10 Nm.

Figure IV-7 next page shows the speed waveform for an initial load torque of 0 Nm and then 10 Nm.

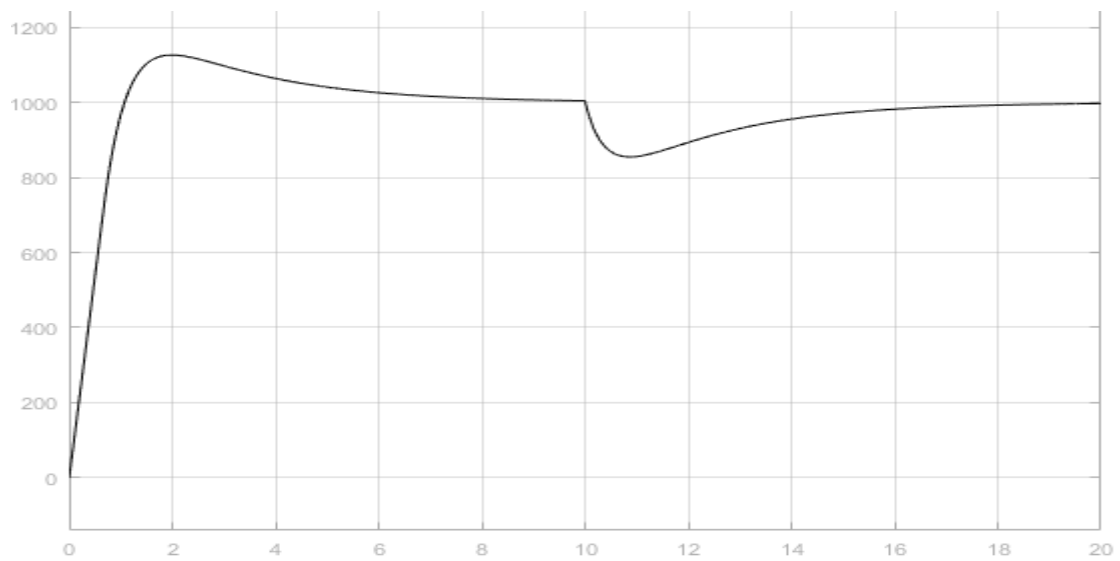


Figure IV-7 speed (rpm) vs time (s) for $T_L=0$ Nm then $T_L=10$ Nm

A field programmable gate array (FPGA) contains a matrix of reconfigurable gate array logic circuitry that, when configured, is connected in a way that creates a hardware implementation of a software application. Sophisticated tools allow the implementation of embedded control systems rapidly and easily and provide limitless flexibility. Unlike hard-wired printed circuit board [PCB] designs that have fixed hardware resources, FPGA-based systems can rewire their internal circuitry to allow configuration after the control system is deployed to the field. Consequently, FPGA based control systems has become the most favourable choice for prototyping digital control systems [5] [6].

V.1FPGA hardware blocks:

The hardware blocks implemented inside the FPGA board are described in VHDL. Quartus II 9.1sp2 Web Edition was used for building these blocks.

V.1.1 ADC block:

The ADC block task is to read the digital data provided by the ADC hardware chip and at the same time to feed the PI and the 7 segments display blocks.

Figure V-1 shows the corresponding ADC VHDL block.

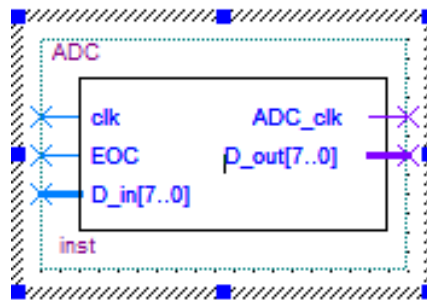


Figure V-1. ADC VHDL block

The block consists of the inputs **clk**, which is the 50 MHz clock, provided with the DE2 FPGA board, **EOC** signal that comes from the ADC hardware chip it goes high at the end of the conversion and allows the FPGA to read the new converted data. The output signal **ADC_clk** is the sampling rate, which is the frequency at which the ADC samples the input analogue signal.

V.1.2 PWM block:

In order to control the speed of the DC motor, PWM technique is used in this project. A PWM device was implemented within the FPGA. A set of specific pulses are generated by the PWM block to drive the H-bridge integrated circuit that is driving the DC motor.

Figure V-2 shows the corresponding PWM VHDL block.

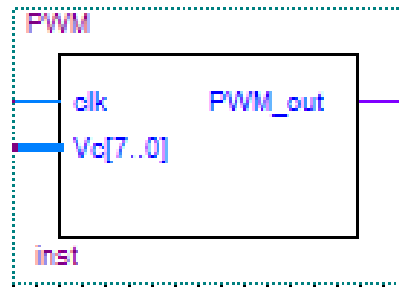


Figure V-2. PWM VHDL block

The 8-bit input **V_C** is the control signal coming from the PID controller, which determines the duty cycle of the output pulses is compared with an 8-bit internal counter. If the internal counter value is less than the value of the control signal **V_C**, the **PWM_out** signal will be high. Otherwise, it will be low.

The flowchart of the PWM is shown in figure V-3 next page.

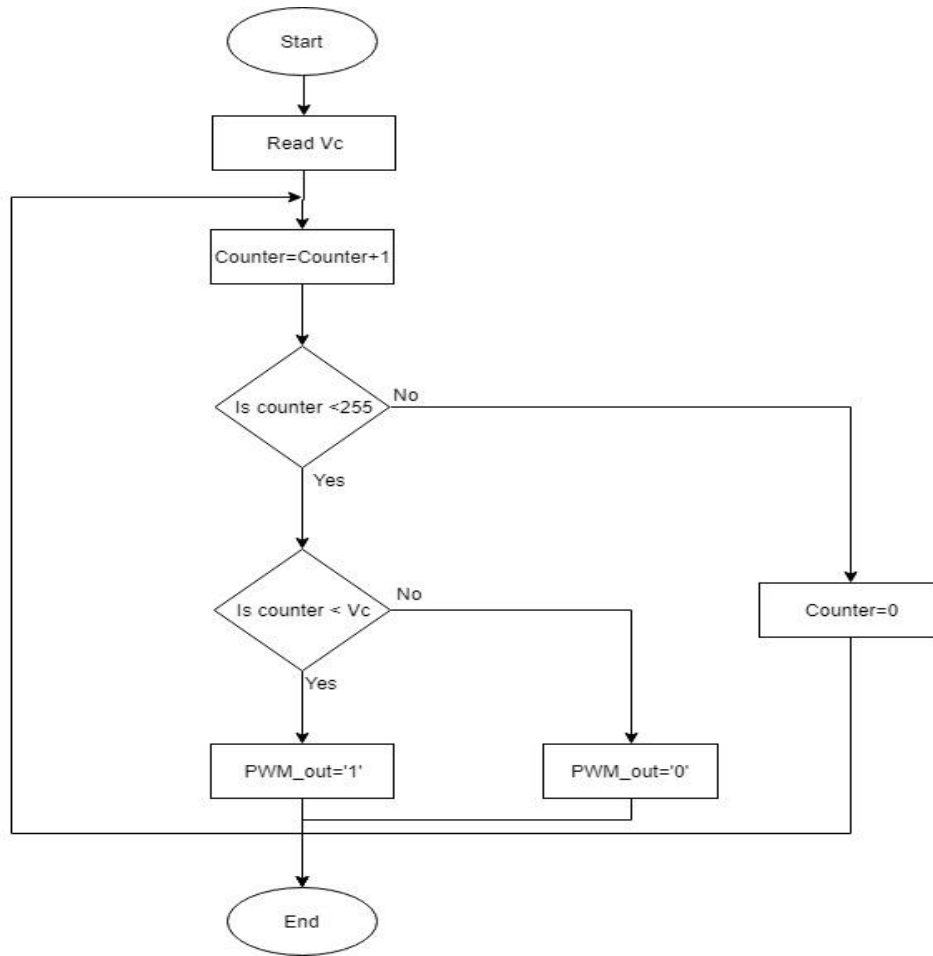


Figure V-3. PWM flowchart

V.1.3 PID algorithm:

The execution of the PID algorithm is performed in the following steps:

1. Set the values of the PID gains (K_P , K_I , K_D) and initialize the signal Error_old.
2. Calculate the new error where:

$$Error = Reference - Measured_value.$$

3. Calculate the PID parameters P, I, and D where

$$P = Error, \quad I = I + (Error * dt) \quad \text{and} \quad D = (Error - Error_{old})/dt.$$

4. Calculate the new output :

$$Output = K_P * P + K_I * I + K_D * D.$$

5. Keep the output within the 8-bit range.

The flowchart of the PID algorithm is shown in figure V-4.

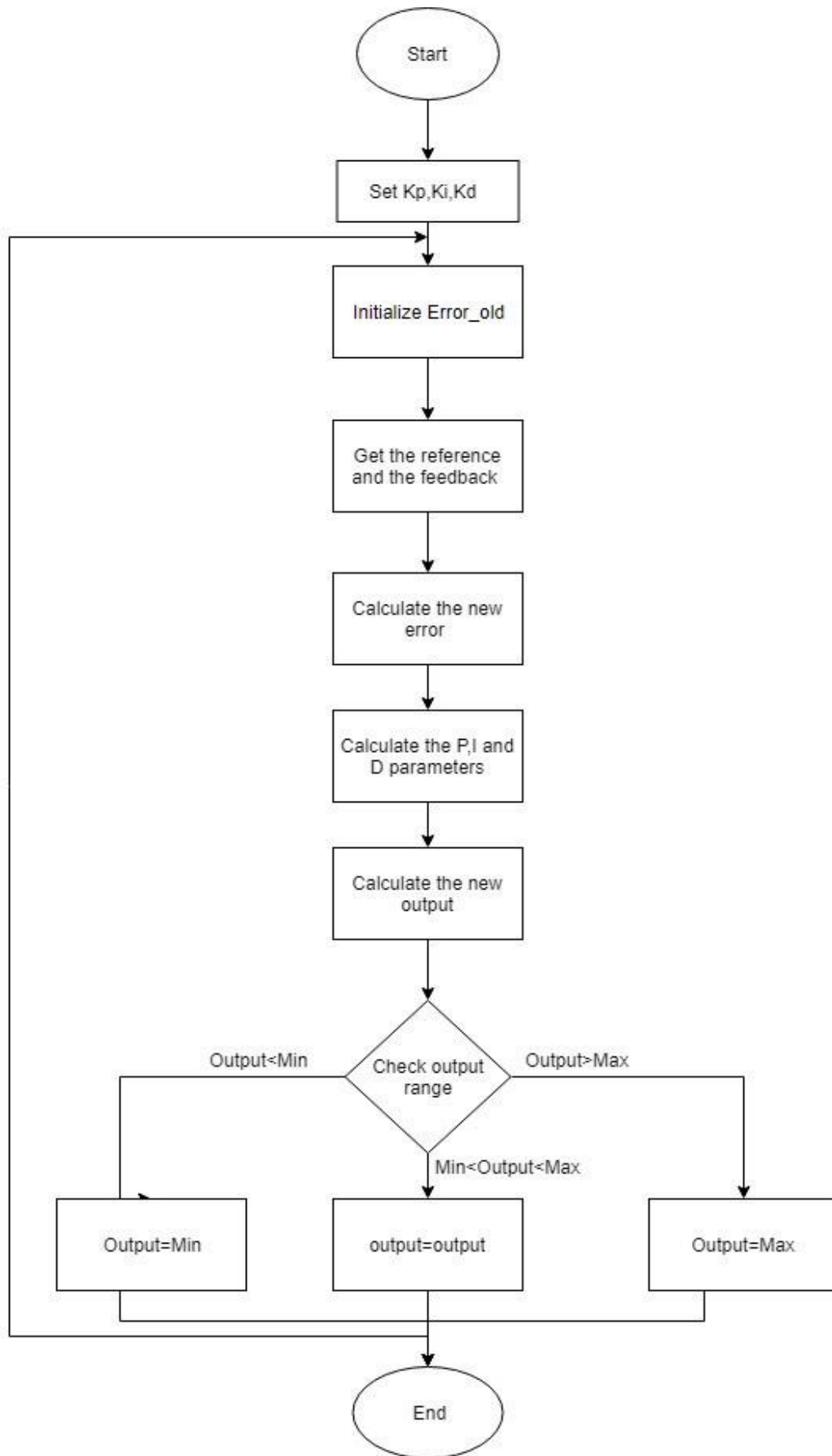


Figure V-4. PID flowchart.

V.1.4 Clock divider block:

The internal clock provided with the FPGA board consists of a 50 MHz clock. Therefore, whenever a lower frequency clock is needed, a clock divider is used. In our project, the clock divider is needed to drive the 7-segment display because the human eye cannot observe the data being displayed at high frequency, and for the PWM because of the H_bridge frequency limit. Figure V-5 shows the corresponding clock divider VHDL block.

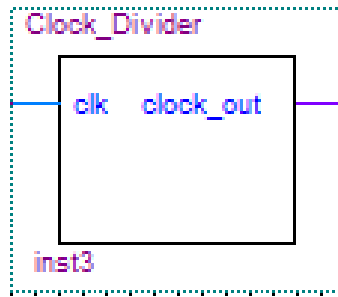


Figure V-5. Clock divider VHDL block

V.1.5 Seven segment display block:

The task of this block is to display the speed of the motor data provided by the ADC in the seven segment display of the FPGA board. Figure V-I shows the corresponding seven segment display VHDL block.

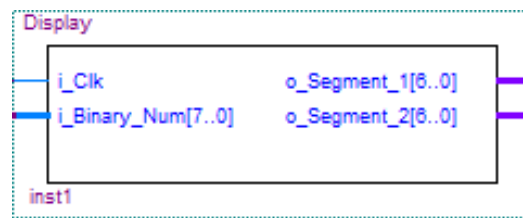


Figure V-6. Seven segment display VHDL block.

Then, all the previous VHDL blocks are Integrated in the FPGA board and connected between them to implement the controller software. The controller software embedded within the Altera DE2 board calculates the required duty cycle and generates the PWM signals for the H_bridge driver through the PWM block using the PID algorithm implemented in the PID block. The speed of the DC motor is maintained at the selected reference. The interconnection between the different blocks is shown in figure V-7.

V.2 Off board design:

V.2.1 The actual speed and current acquisition:

The speed of the DC motor and the armature current need to be converted into electric voltage in order to be manipulated. For the motor speed, a tachogenerator can be used to convert the speed, which is a mechanical quantity into an electrical quantity that is voltage.

In the same way, the armature current of the DC motor needs to be converted to a voltage, because the input of the next stage (analog to digital converter) has to be voltage, therefore a current transducer is needed.

The most simple and economic current transducer is a shunt resistor, the voltage across the resistor is function of the current flowing through it. However, adding an external resistor can affect the parameters of the motor. Consequently, the controllers will be affected and the control system response will change.

The solution is to use a Hall Effect current transducer such as the LA 25–P, which has an excellent accuracy, the current in the primary is proportional to the current in the secondary. The current that flows in the primary of the Hall Effect sensor is the armature current. The secondary current must be passed through an external measurement resistor so that the voltage across the resistor is function of the armature current, this resistor is selected such as: $R_m = \frac{V_{ref}}{I_r}$ where V_{ref} is the reference voltage given to the ADC chip and I_r is the rated armature current of the motor.

V.2.2 Analog to digital conversion:

The actual speed and armature current of the DC motor are in analog form. Therefore, they need to be converted to digital form using an analog to digital converter to perform further applications.

In our design, two ADC0808 analog to digital converters were used. One for the speed and the other for the armature current. For the speed, the V_{ref+} and V_{ref-} values is set to V_{max} and 0V respectively where V_{max} is the maximum voltage obtained from the tachogenerator which corresponds to the base speed.

For the armature current, the V_{ref+} and V_{ref-} are set to V_{max} and 0V respectively where $V_{max} = I_r * R_m$.

Figure V-8 shows the hardware connections.

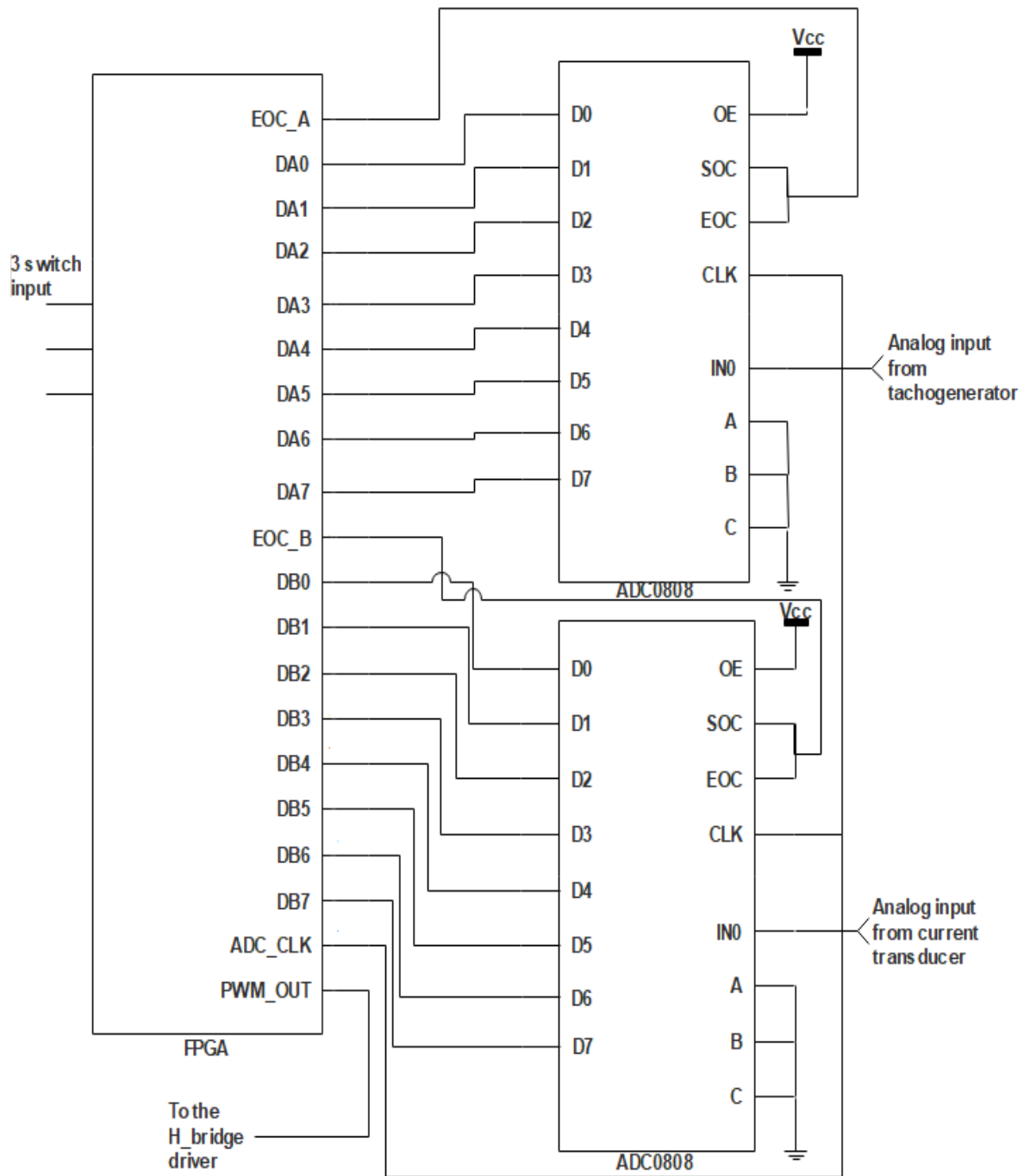


Figure V-8. Hardware system connections.

V.3 Hardware implementation:

Our hardware design was based on controlling a 2KW DC motor but during the process of implementation, we faced a problem, we could not find an H_bridge driver that could support 2KW the only H_bridge that we could find was the L293D integrated circuit. Therefore, we decided to carry out the implementation using a small DC motor that can be driven by the L293D driver.

V.3.1 Experimental setup :

The experimental setup is shown in figure V-10. The three input switches are used to select the reference speed 25%, 75% and 100% of the base speed. The measured speed and the armature current are converted to digital data by the ADC chips and fed back to the FPGA board through the GPIO ports. The DC motor is driven by the L293D H-bridge depending on the PWM signal coming from the board.

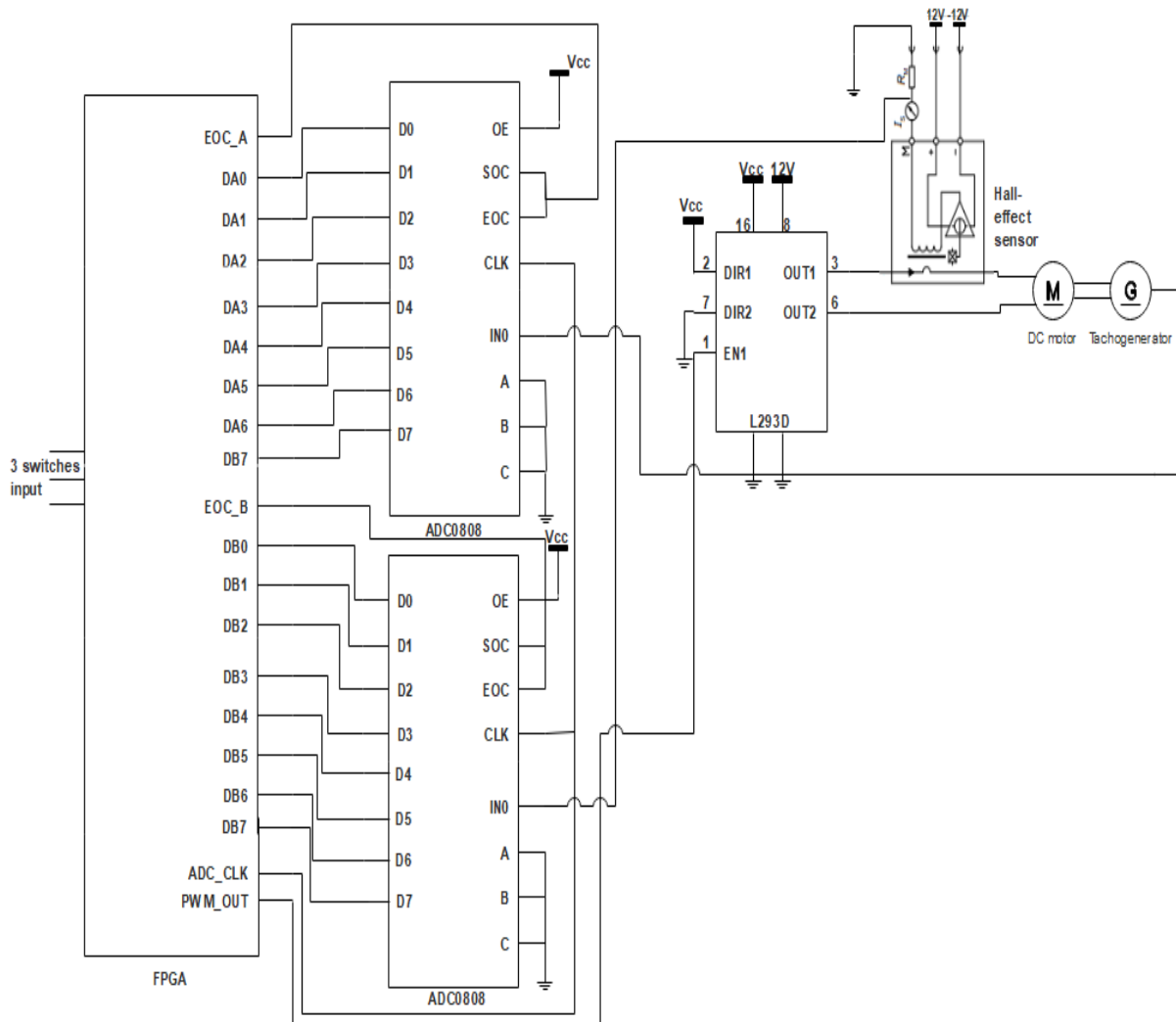


Figure V-9. Experimental setup connections.

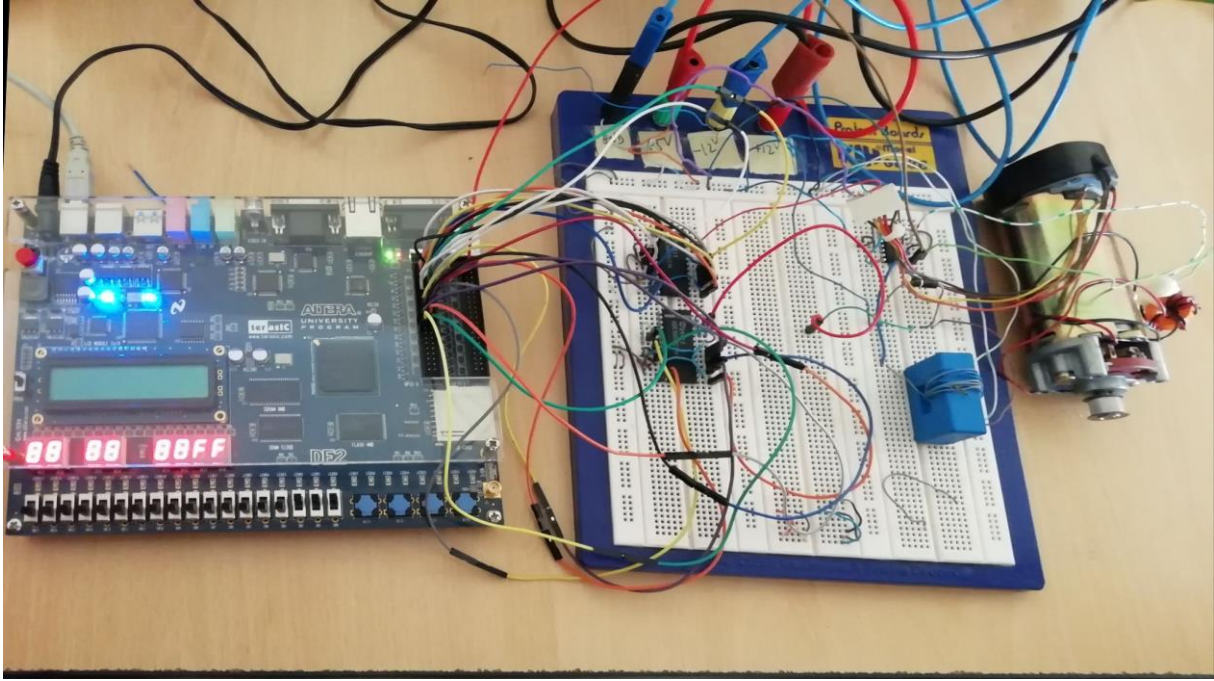


Figure V-9. Experimental setup

V.3.2 Implementation results:

The experiment is conducted to verify the performance of the controller hardware design. The VHDL design was downloaded into the DE2 FPGA board. A reference speed of 25% of the base speed was assigned to the input switches. The ADC blocks read the actual speed and current data from the ADC chips then the PID1 block calculates the control signal for the PID2 block and the PID2 block calculates the control signal that feeds back the motor through the PWM block. The motor started running at the reference speed when the actual speed matches the reference speed as observed from the seven segment display. Then, the same procedure was repeated for reference speeds of 75% and 100% of the base speed. Observed equivalent hexadecimal values of the actual speed which is displayed on the seven segment display and tacho-generator voltage were tabulated in table V-1.

Table V-1. Result of control system for various reference speeds.

Input switches position	Reference speed	Equivalent HEX value	Tacho-generator voltage (V)
000	0% of base speed	00	0 V
001	25% of base speed	40	0.8V
011	75% of base speed	C0	2.5V
111	100% of base speed	FF	3.3V

To show the control system response, the first speed (25% of base speed) is assigned to the input switches and then a scope is used to plot the waveform of the tacho-generator voltage as shown in figure V-10.

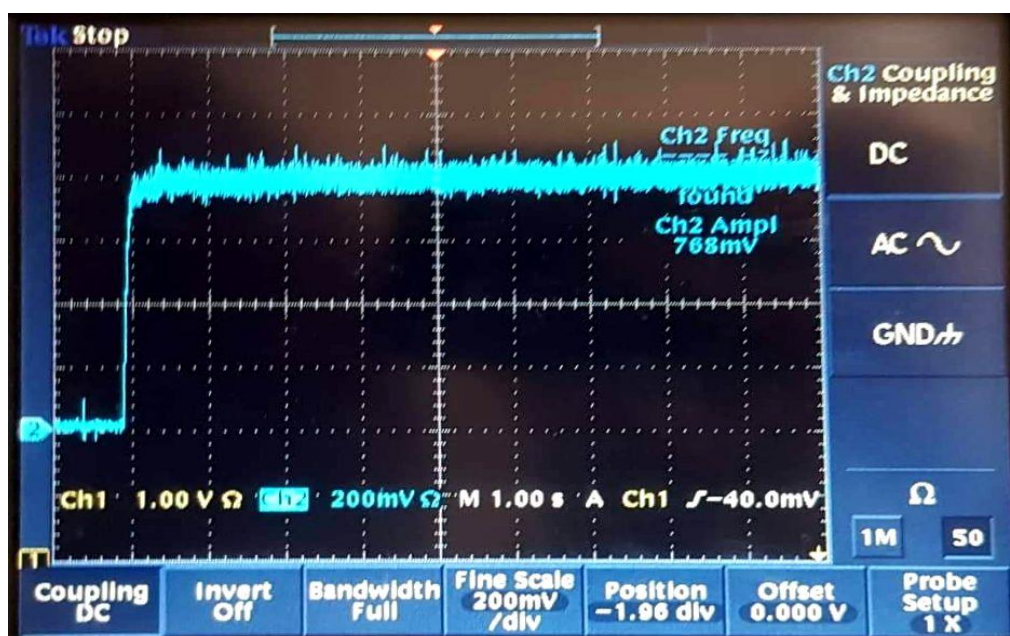


Figure V-10. Measured tacho-generator voltage (speed) vs time.

From the above figure, the result of the control system response showed a noisy behavior. This is due to the steady state error and also due to the tacho-generator. It can be observed that the tacho-generator signal is noisy even when the speed was set to zero and the motor was not revolving.

General Conclusion

The main objective of this project is to control the speed of a separately excited DC motor; as seen in this report many methods of controlling the speed and the torque has been discussed briefly, however, the armature voltage control technique has been presented in details.

The simulation of this control technique has been done on a 2 kW motor. However, the prototype implementation of the armature voltage technique was carried on a small DC motor due to the absence of an H-bridge that can support a 2 kW power.

As said previously in the report, controlling the speed and the torque of a DC motor using the armature voltage controlling method is widely used in the world of electricity and electronics due to its simplicity and efficiency. In this project, an FPGA board has been used to control this speed and torque. FPGA has been chosen due to our familiarity with the VHDL, its robustness and the ease of control.

From this project, we have learnt the difference between implementing and simulating system, in fact, the difficulties that may be faced during the implementation and the experiment and hence the challenges we had led us to acquire a wide knowledge of the DC motors such as their working principle, behaviour with digital controllers and their speed and torque control.

References

- [1] Stephen J Chapman. *Electric machinery fundamentals*. 4th edition. Published by McGraw-Hill, New York, 2004.
- [2] [https://en.m.wikipedia.org/wiki/chopper_\(electronics\)](https://en.m.wikipedia.org/wiki/chopper_(electronics)). (accessed on 11/06/2019).
- [3] Pr. A.Khaldoun. *EE533- Machines and drives*. Chapter III: Variable voltage fed DC motors. Fall 2016.
- [4] "Sizing a Grid-Tied PV System with Battery Backup Home Power Magazine". www.homepower.com. (accessed on 14/06/2019).
- [5] A.de castro, P.Zumel, D.Garcia, J.Uceda. *Concurrent simple digital controller of an AC/DC converter with power factor correction based on FPGA*, IEEE Trans. Power electronics. Vol. 18pp. 334 343 , 2003.
- [6] Y. F. Chan, M.Moallem, W. Wang. *Efficient implementation of PID controller algorithm using FPGA technology*. Proceedings of the 43 ed IEEE conference on decision and control, V5, PP. 4885-4890, Bahamas 2004.

Appendix A

The L293D dual H-bridge integrated circuit motor driver.

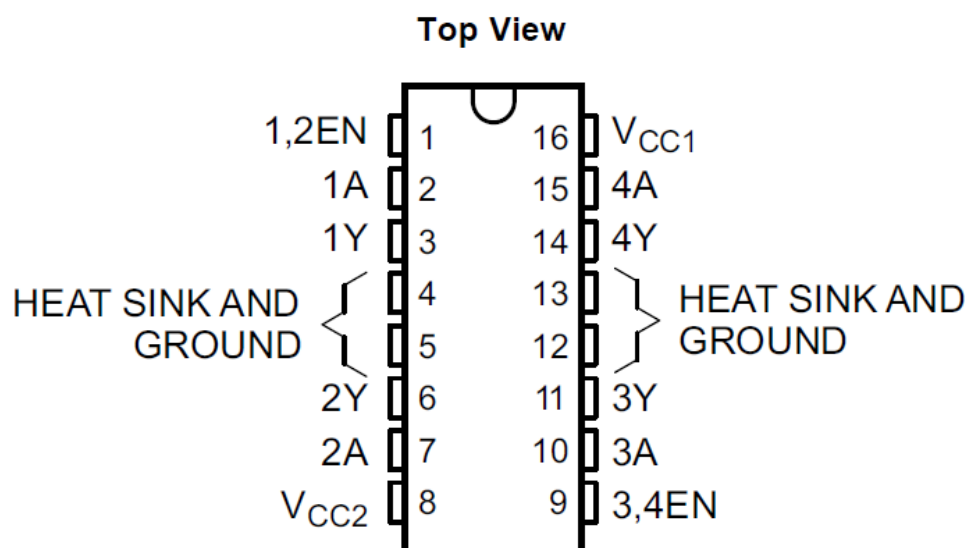


Figure A-1. Pin diagram of the L293D H-bridge

The 8-bit analog to digital converter ADC0808.

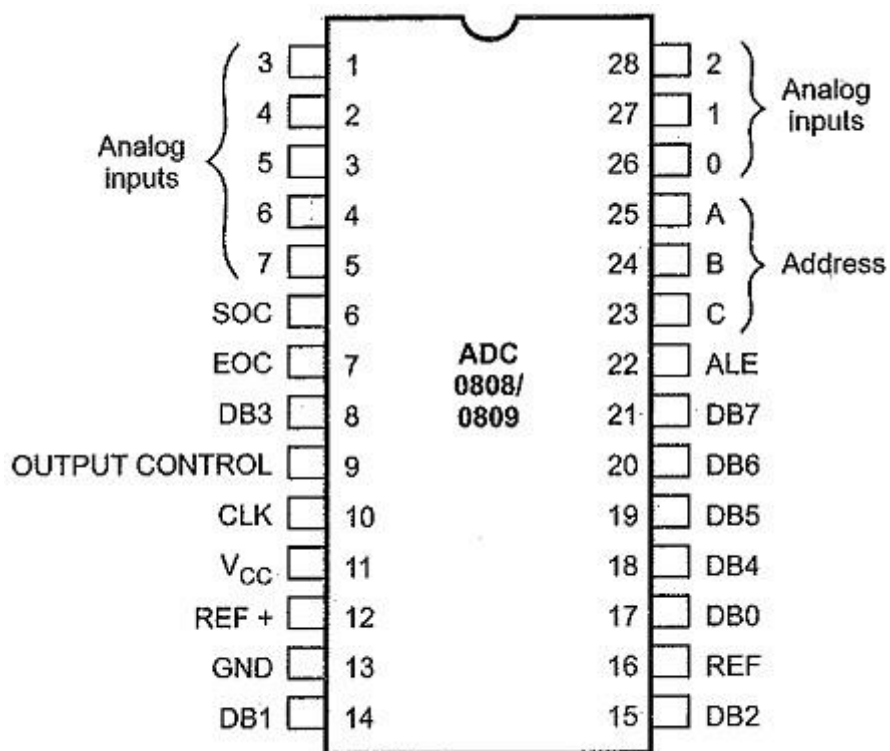


Figure A-2. Pin diagram of ADC0808

